INL/RPT-22-66727

Gamma Irradiation of NaCl-UCl_3 Salt for the Molten Chloride Fast Reactor

May 2022

Final Report

William Phillips
Guoping Cao
Stephen Warmann
Brennan Mohr
Evan Lovel
Gregory Core

Idaho National Laboratory

INL is a U.S. Department of Energy National Laboratory operated by Battelle Energy Alliance, LLC

INL/RPT-22-66727

Gamma Irradiation of NaCl-UCl3 Salt for the Molten Chloride Fast Reactor

Final Report

William Phillips
Guoping Cao
Stephen Warmann
Brennan Mohr
Evan Lovel
Gregory Core

May 2022

Idaho National Laboratory
Idaho Falls, Idaho 83415

http://www.inl.gov

Prepared for the
U.S. Department of Energy
Office of Nuclear Energy
Under DOE Idaho Operations Office
Contract DE-AC07-05ID14517

Page intentionally left blank

ABSTRACT

This report documents the results of the gamma ray irradiation of NaCl-UCl_3 eutectic salt in the Advanced Test Reactor (ATR) spent fuel pool gamma tube and subsequent analysis of capsules utilizing the Gas Assay Sample and Recharge (GASR) system. NaCl-UCl_3 salt capsules at four different temperatures, 75°C to 131°C, 150°C, 300°C and 600°C, were irradiated shortly after the core internal changeout (CIC) of the ATR, beginning April 28th of 2021, and ending on August 18th of 2021. Gamma heating of the low temperature capsule resulted in the experimental temperature of this capsule remaining above the target 75°C set point for a significant portion of the experiment. Re-positioning of the fuel elements in the spent fuel pool to move more fresh fuel elements around the gamma tube occurred on May 11th of 2021, resulting in an approximate 20% increase in the dose rate. In total, the salt-filled capsules underwent 2638 hours of gamma irradiation and accumulated approximately 31 MGy of total absorbed dose from the adjacent freshly discharged ATR spent fuel. Capsule internal pressure measurements were taken via the Gas Assay Sample and Recharge (GASR) system in the INL Hot Fuels Examination Facility (HFEF) following completion of the irradiation. Based on the GASR analysis results, the primary conclusion from this experiment to-date is that radiolytic generation of chlorine gas is insignificant for the dose rates and total absorbed dose that these samples experienced. To elucidate more detailed effects of radiolysis on NaCl-UCl_3 eutectic salts and reach a more definitive conclusion, further advanced analyses such as electron microscopy, simultaneous thermal analysis, and electron paramagnetic resonance are recommended to analyze the capsule wall and salt samples.

Page intentionally left blank

CONTENTS

FIGURES

TABLES

Page intentionally left blank

ACRONYMS

ATR: Advanced Test Reactor

CIC: Core Internals Changeout

CRADA: Cooperative Research and Development Agreement

DSC: Differential Scanning Calorimetry

ECAR: Engineering Analysis and Calculation Report

EDS: Energy Dispersive X-ray Spectroscopy

EPR: Electron Paramagnetic Resonance

FMF: Fuel Manufacturing Facility

GASR: Gas Assay, Sample and Recharge

GCMS: Gas Chromatography–Mass Spectrometry

HFEF: Hot Fuel Examination Facility

ICP-MS: Inductively Coupled Plasma Mass Spectrometry

INL: Idaho National Laboratory

MCFR: Molten Chloride Fast Reactor

MFC: Materials and Fuels Complex

MCRE: Molten Chloride Reactor Experiment

MSRE: Molten Salt Reactor Experiment

PIE: Post-Irradiation Examination

SEM: Scanning Electron Microscopy

STA: Simultaneous Thermal Analyzer

TREAT: Transient Reactor Test Facility

Gamma Irradiation of $NaCl\text{-}UCl_3$ Salt for the Molten Chloride Fast Reactor

1. Introduction

Based on the limited available literature data, radiolysis of chloride salts is expected in the spent fuel salts from the TerraPower Molten Chloride Fast Reactor (MCFR). Such radiolysis can generate corrosive Cl_2 gas and subsequently HCl if moisture is present. The radiolysis of solid salts is found to be affected by the total absorbed dose, dose rate, quantity of salt impurities, and temperature [1–11]. Significant experience has been gained from the radiolysis of fluoride salts in the Molten Salt Reactor Experiment (MSRE) [12–17], but experimental radiolysis data is lacking that directly applies to long-term storage of spent MCFR salts. Consequently, systematic studies are needed to understand the radiolysis behavior of solid chloride salts in prototypical MCFR spent fuel radiation environments.

It is generally accepted based on the experience gained during the MSRE that chloride salts may be thermodynamically and radiolytically stable in the operating conditions of the MCFR and that no net radiolysis in molten chloride salts is expected. Nevertheless, the understanding of radiation damage in molten chloride salts is limited and the immunity of molten chloride salts to radiolysis cannot be assumed. A recent report by Brookhaven National Laboratory concluded that "For fast spectrum chloride salts, there is a need for high flux radiation stability tests to determine if radiolysis effects are significant…The radiolysis of the salts could affect the composition of the salts and lead to formation of corrosive gaseous products such as chlorine gas. The rate of radiolysis and recombination is currently not known and needs experimental evaluation" [18]. Because chloride salts have not been tested under conditions similar to the intense radiation environment present in the MCFR, which may be significantly different from those in the fluoride salt fueled, thermal spectrum MSRE, experiments will be needed to confirm the radiolytic stability of chloride salts for industrial application in the MCFR.

To address the above knowledge gaps an initial gamma irradiation experiment was performed in the Advanced Test Reactor (ATR) gamma tube using $NaCl\text{-}UCl_3$ eutectic salt at four different temperatures. The $NaCl\text{-}UCl_3$ eutectic salt is being considered as a candidate fuel salt for development of demonstration reactors and the MCFR. This report documents the experimental details, results to-date, and ongoing work for this gamma irradiation experiment.

2. Experimental

2.1 ATR Gamma Tube

The ATR gamma tube No. 3 (as shown in Figure 1) is a 20.5 ft. vertical tube that has a usable inner diameter of 5 in. and a usable length of 19 ft 8 in. from the top to the lead shielding at the bottom. The tube is fabricated out of schedule 10 stainless steel. The intensity of the gamma irradiation dose rate depends on the irradiation history, age, and proximity of the fuel to the gamma tube. An as-measured typical gamma field value in the gamma tube with ATR fuel

elements, freshly removed from the reactor, and placed adjacent to the gamma tube, is 5×10^6 rad/hr. Gamma-ray intensity will fall off at a rate of approximately 5% per day as the fission products in the fuel elements decay. The typical neutron source strength in the gamma tube with fresh ATR fuel elements is 300 n/cm^2/s. Figure 2 shows ATR gamma tube field measurements taken over time.

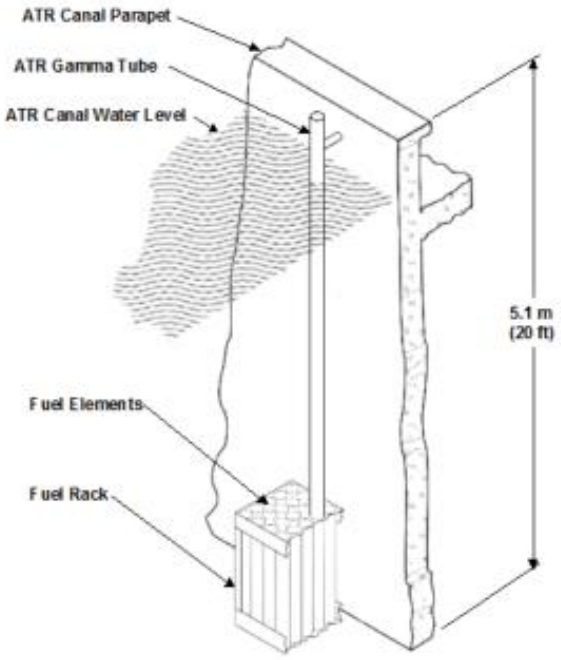

Figure 1. Schematic of ATR gamma tube No.3

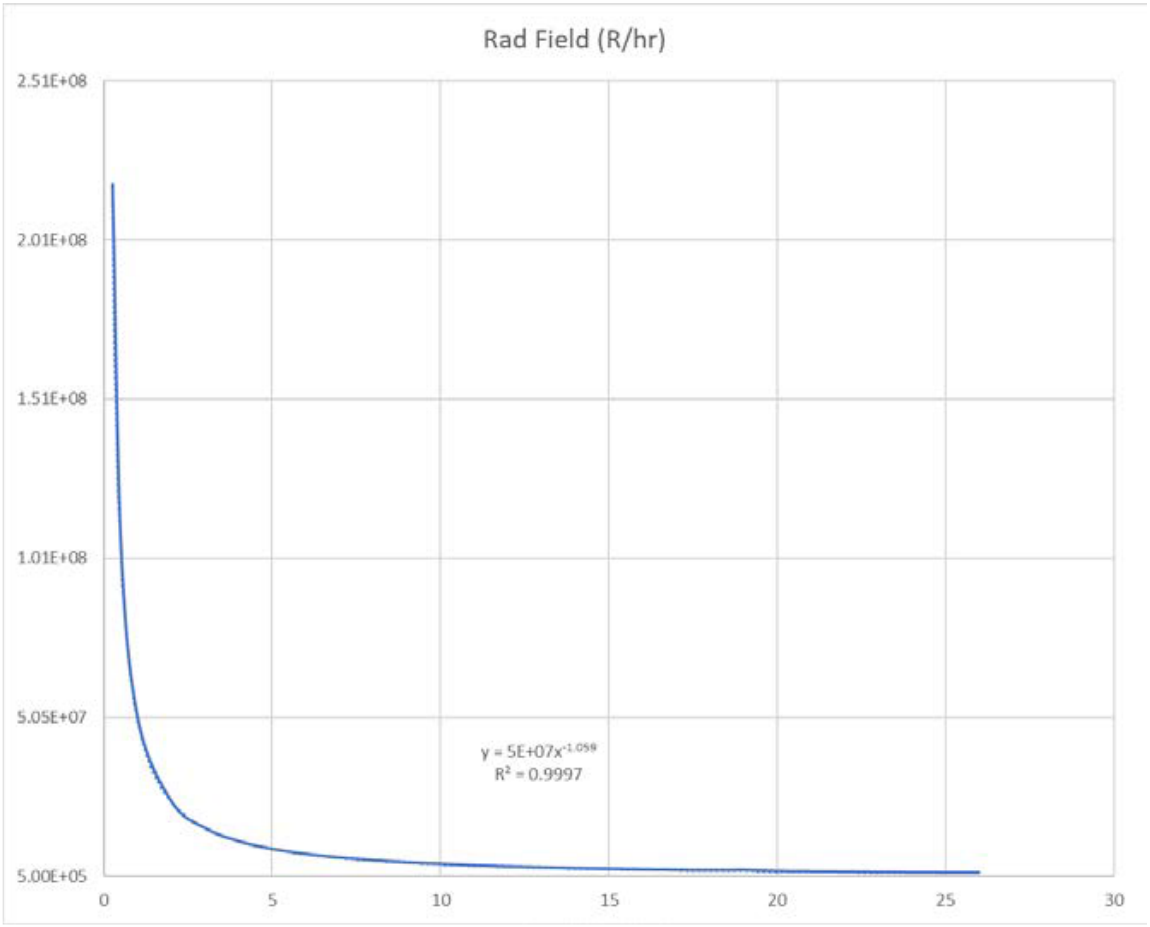

Figure 2. Typical calculated dose rate of the ATR gamma tube versus time (days)

2.2 Test Matrix

Table 1 lists the basic conditions for the gamma irradiation of NaCl-UCl_3 salt, including salt composition, test temperatures and dose rates. The salt mixture is a 67NaCl-33UCl_3 (in mol%) salt, which is a eutectic salt with a melting point of 524 °C. Test temperatures of 75, 150, and 350 °C were selected for solid salt radiolysis experiments, and 600 °C was selected for liquid salt radiolysis testing. 600°C is approximately 80 °C higher than the liquidus temperature of eutectic NaCl-UCl_3 salt and is the lower temperature for reactor operation. Sealed capsules were used for the irradiation. Due to the space constraints of performing multiple tests simultaneously in the ATR gamma tube, only one capsule at each temperature was used. It should be noted that the experiment was initially designed around the use of NaCl-$PuCl_3$ eutectic salt, as this was the fuel of choice for TerraPower's Molten Chloride Reactor Experiment (MCRE) at the time. This resulted in significant design limitations due to Pu handling and transportation restrictions. The pivot to NaCl-UCl_3 salt for MCRE led to the NaCl-UCl_3 eutectic salt being selected for this experiment. The change to uranium did not result in delays to the experiment schedule as the requirements for handling plutonium bound those required for handling uranium, however, if the experiment had been designed from the outset around the requirements necessary to handle depleted uranium instead of plutonium, the capsule volume, salt volume, number of samples, and gas analysis techniques could have been optimized to simplify the challenges associated with detection of chlorine.

Table 1. Salt composition and test conditions for gamma irradiation

Salt	Irradiation temperatures	Irradiation conditions Dose rate, dose, time
67NaCl–33UCl_3 (mol%)	Solid salt 75°C, 150°C, 350°C	Medium dose rate, Less than 5×10^6 rad/hr
67NaCl–33UCl_3 (mol%)	Liquid salt 600°C	Medium dose rate, Less than 5×10^6 rad/hr

2.3 Preparation of NaCl-UCl_3 Salt

The NaCl and UCl_3 used for this experiment were both provided by TerraPower. Prior to fusing the NaCl and UCl_3 into the eutectic composition, the NaCl was dried under vacuum in an Ar atmosphere glovebox for 4 hours at 400°C. TerraPower prepared the pure UCl_3 via their proprietary hydride-hydrochlorination process. No further purification of the UCl_3 was performed at INL. After transferring the feedstock salts into the argon-atmosphere Advanced Fuel Cycle Initiative (AFCI) glovebox within the Fuel Manufacturing Facility (FMF) at the Materials and Fuels Complex (MFC), 29.557g of UCl_3 was blended with 10.093g of NaCl in a glassy carbon crucible and covered with a glassy carbon lid. The crucible containing the blended salts was then heated at 5°C per minute to 820°C, starting from 20°C. The furnace was held at temperature for 1 hour and then allowed to cool overnight. After the salt was cooled, the fused NaCl-UCl_3 ingot was removed from the crucible and broken into small pieces, followed by grinding using an agate mortar and pestle. Large particles were periodically separated from the fines and re-ground until all particles passed through a 40-mesh sieve. To allow for loading of salt into the capsules, the salt powder was pressed into 8mm diameter pellets using a stainless-steel pellet die set and a hydraulic press. Approximately 1.25g of salt was loaded into the die set and pressed to 2000psi for 1 minute for compaction, resulting in pellets of 8mm in diameter and approximately 5mm in height. Figure 3 shows some photographs of the NaCl-UCl_3 salt preparation process.

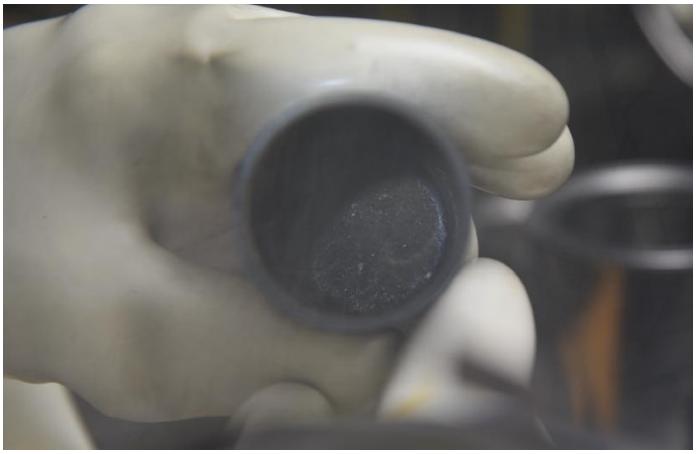

(a)

(b)

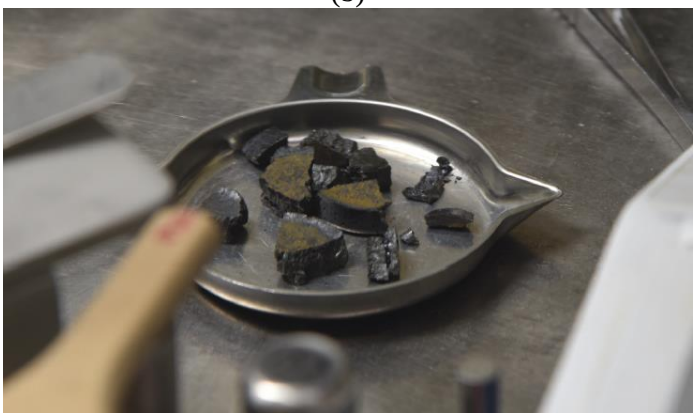

(c)

(d)

(e)

Figure 3. Photographs showing the process of NaCl-UCl_3 salt preparation: (a) salt solidified in a glassy carbon crucible, (b) salt ingot removed from glassy carbon crucible, (c) salt pieces broken from ingot, (d) salt powders ground using mortar, and (e) salt pressed into pellets, ready for loading into capsules.

2.4 Design and Preparation of Salt Capsules for Gamma Irradiation

The salt capsules consisted of NaCl-UCl_3 eutectic salt sealed in a nickel based alloy 625 type 2 tube (3/8" dia. OD, 0.020" wall, and 3.0" long) with both ends sealed with plugs via gas tungsten arc welding under welding procedure I4.0. Figure 4 shows photographs of a nickel alloy 625 tube and two end plugs used for fabricating the salt capsules. After the bottom of the alloy 625 tube was welded and inspected, five NaCl-UCl_3 pellets were loaded into each capsule then the top of the tube was pressed in place and welded to seal the capsule. The pellets chosen for each capsule were selected by weight to result in similar salt loadings for each capsule.

A tube heater with temperature control and thermal insulation was used to heat the capsules to the test temperature. An aluminum alloy holder was used to house the salt capsules, heaters, and insulation. A schematic of the salt capsules and two photographs of a capsule and capsules assembled are shown in Figure 5 and Figure 6 respectively. All the salt capsules were prepared and welded in FMF at MFC, and then transferred to ATR.

(a)

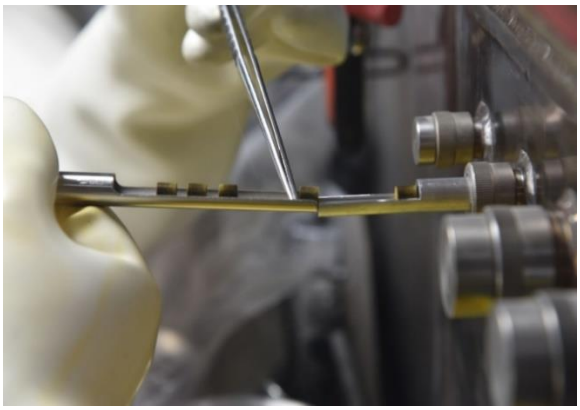

(b)

(c)

(d)

Figure 4. Photographs showing the parts for a salt capsule, salt loading, and fabrication of the salt capsule by weld sealing. (a) Alloy 625 tube and two end plugs, (b) salt loading, (c) preparation for weld sealing, (d) a completed weld sealed salt capsule

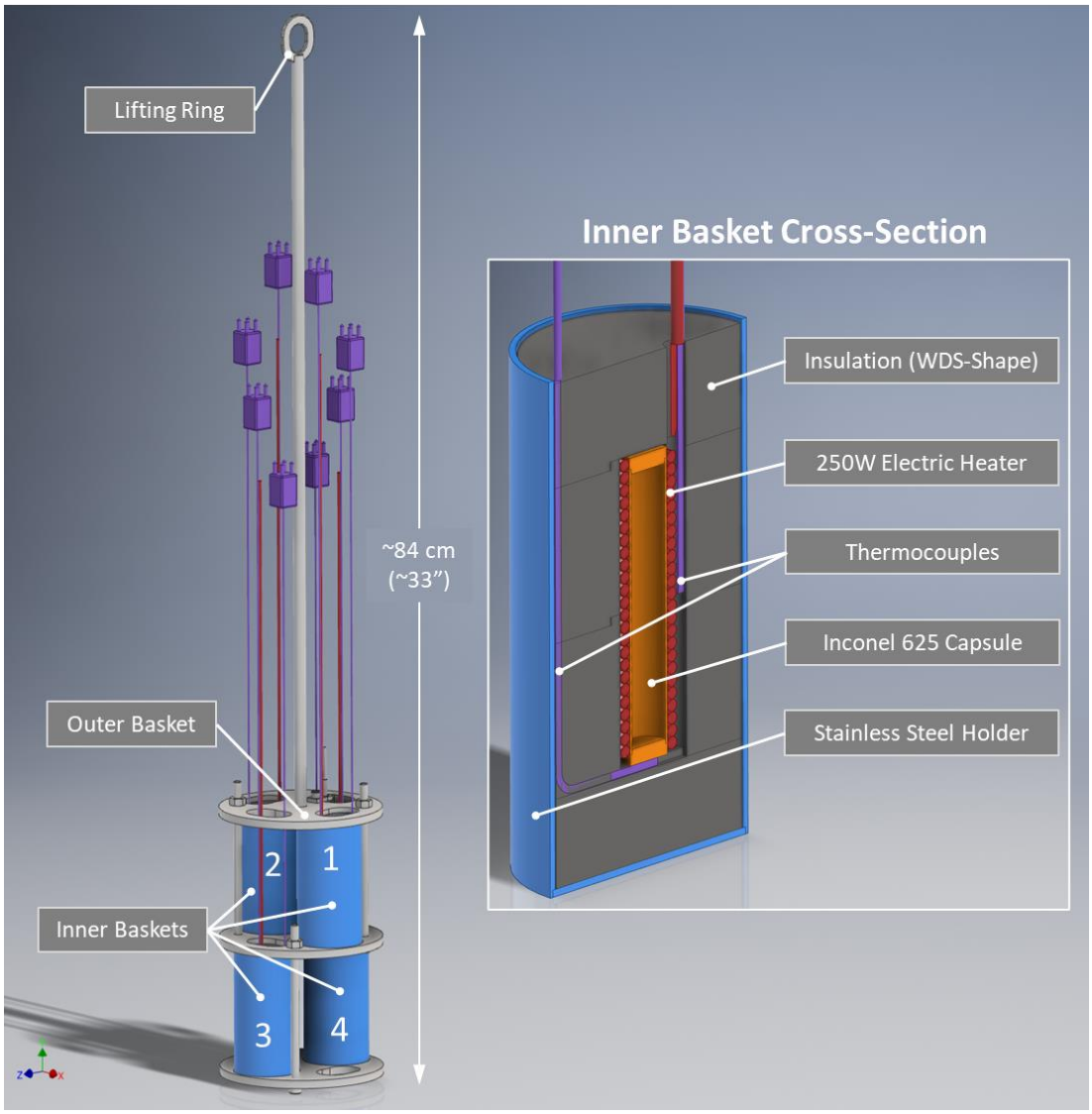

Figure 5. Schematic of the salt capsule with heater and thermal insulation material

Figure 6. Photographs of a capsules and the experiment assembly prior to NaCl-UCl_3 capsule loading.

To ensure the outside temperature of the capsules during the gamma irradiation met the safety requirements of the ATR gamma tube, an engineering analysis and calculation report (ECAR) was performed. The ECAR concluded that the temperatures of the gamma tube components would only be negligibly affected by the expected range of experiment temperatures. The details of the ECAR are provided in Appendix A.

2.5 Gamma Irradiation Test

After the salt capsules were transferred to ATR, they were assembled with the experiment apparatus. An Exadrin A12 ion chamber was also installed near the salt capsules+ assembly to monitor, in real time, the dose rate during testing. The dose and dose rate were recorded using a SuperMax Electrometer. The function of the thermocouples and heaters, along with the data acquisition system, was tested and confirmed before the salt capsules were loaded into the ATR gamma tube. Figure 7 shows photographs of the power supply and temperature control and data-logging system for the gamma irradiation test. After successful demonstration of the temperature control and data-logging, the salt capsules were then loaded into the ATR gamma tube on April 28th, 2021.

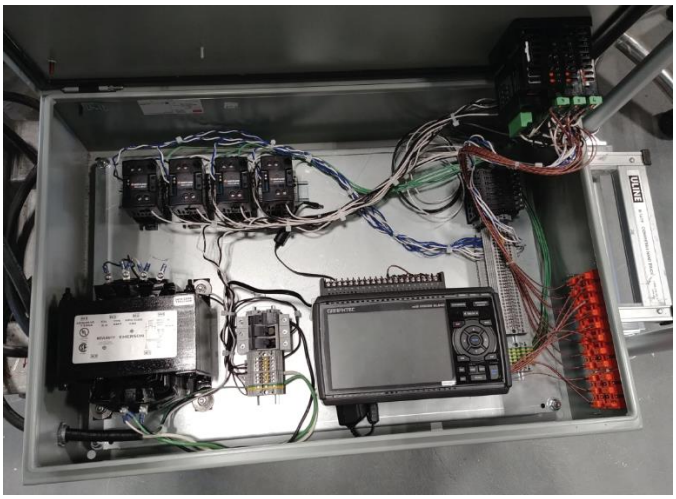

(a)

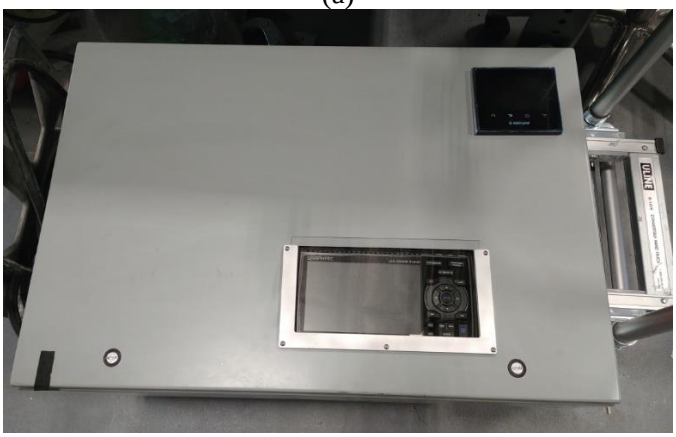

(b)

Figure 7. Photographs of power supply, temperature control, and data-logging system for the gamma irradiation. (a) with cover removed showing the internal components and (b) with cover installed.

3. Results

3.1 Timeline and Insertion of Salt Capsules into the ATR Gamma Tube

ATR CIC completed on April 25, 2021 resulting in freshly spent fuel being positioned around the gamma tube. The gamma irradiation test was inserted into the gamma tube on April 28th, 2021 at 11:05 AM and was removed on August 18th, 2021 at 9:20 AM. Additionally, on May 11th beginning at 8:00 AM, fuel assemblies were shuffled in the spent fuel pool to increase the dose rate on the samples. Limitations on the dose rate experienced by the spent fuel pool concrete walls prevent fresh fuel from being placed within the two rows closest to the wall before 14 days after reactor shut down. The total duration for the gamma irradiation was approximately 2638 hrs. Figure 8 and
Figure 9 show photographs taken at ATR showing preparation of the salt capsules assembly and the process of the inserting the salt capsules into the ATR gamma tube. Figure 10 shows the control panel for controlling the heaters for the salt capsules and logging the temperature during the duration of the gamma radiation test. The status of the test was periodically monitored and no problems associated with the heaters were observed. However, both the ion chamber and electrometer used to measure and record dose rate data suffered failures several weeks into the irradiation. The USB port on the electrometer failed in late June rendering the data recorded after that point irrecoverable, however, by that time, the ion chamber had degraded to the point of failure, meaning that the failure of the electrometer was inconsequential. The computer used for data logging the temperature data crashed once during the test on June 9th, likely due to an overflow error caused by the large amount of data stored over the preceding 6 weeks, however, it did not impact the operation of the control cabinet and did not cause temperatures to deviate from their setpoints. Restarting the computer on June 15th resolved the issue and allowed data collection to resume.

(a)

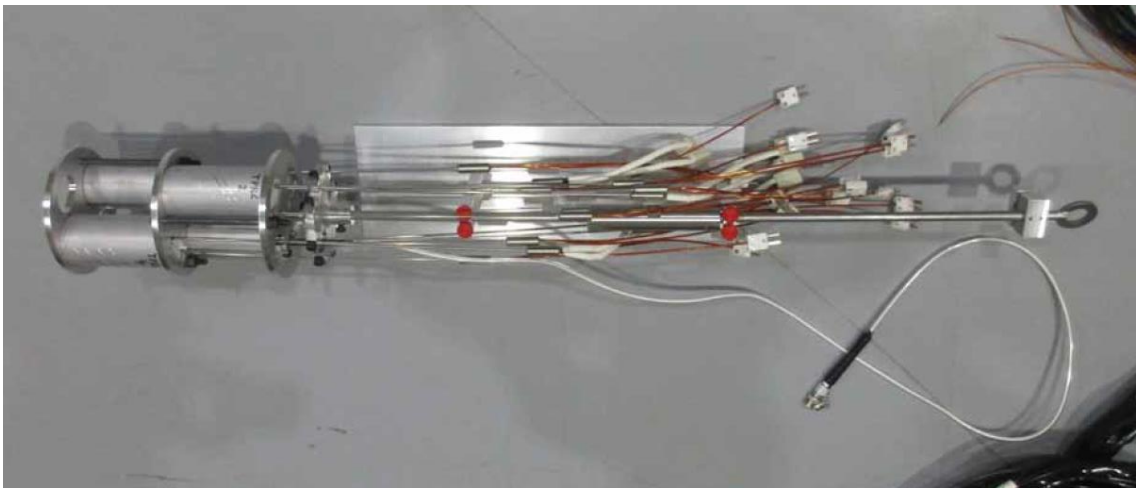

(b)

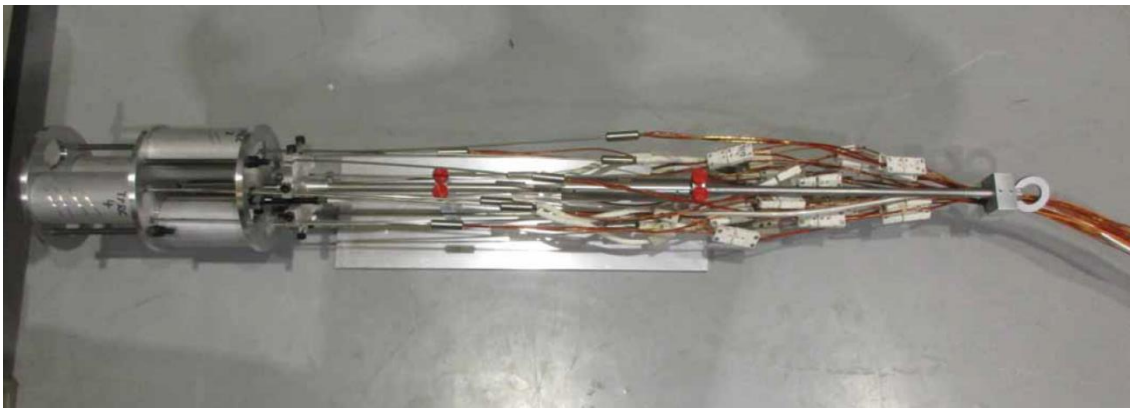

(c)

Figure 8. Photographs showing the process of preparing the salt capsule assembly, (a) salt capsules inserted in coil heaters, (b) Salt capsules assembled, with gamma dose meter inserted, and (c) completed salt capsule assembly ready for insertion into the ATR gamma tube

.

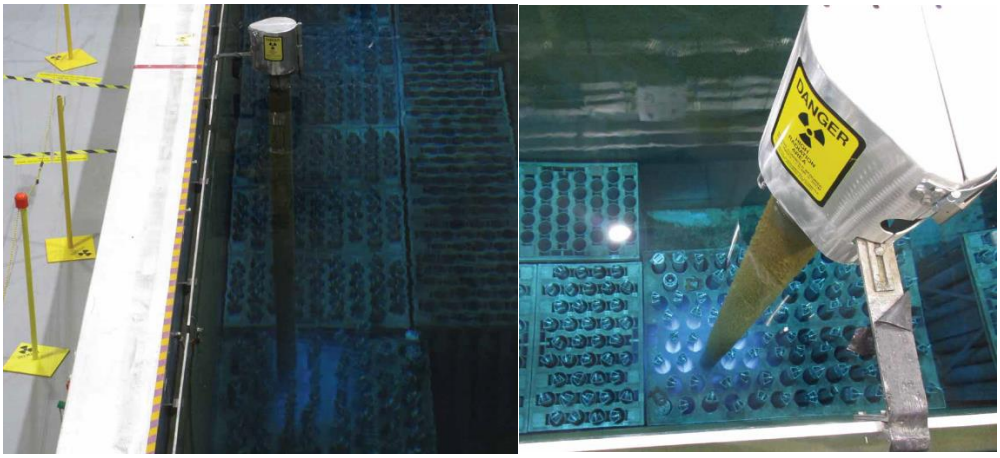

(a)

(b)

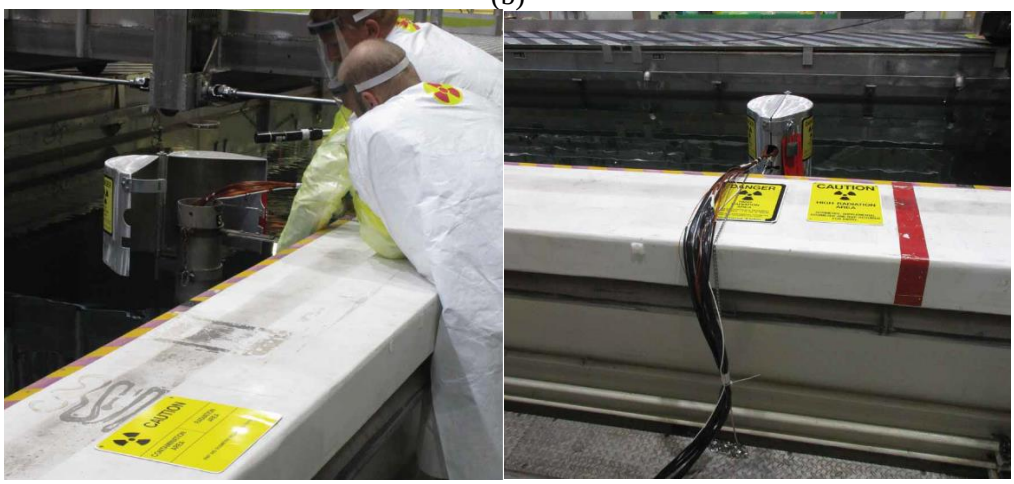

(c)

Figure 9. Photographs taken at ATR showing the process of inserting the salt capsules into the ATR gamma tube. (a) overall pictures showing the gamma tube and spent fuel pool with spent fuel assemblies at the bottom, (b) pictures showing engineers preparing the insertion of the salt capsules into the gamma tube, (c) pictures showing engineers inserting the salt capsules into gamma tube and gamma tube when the insertion of salt capsules is completed.

(a)

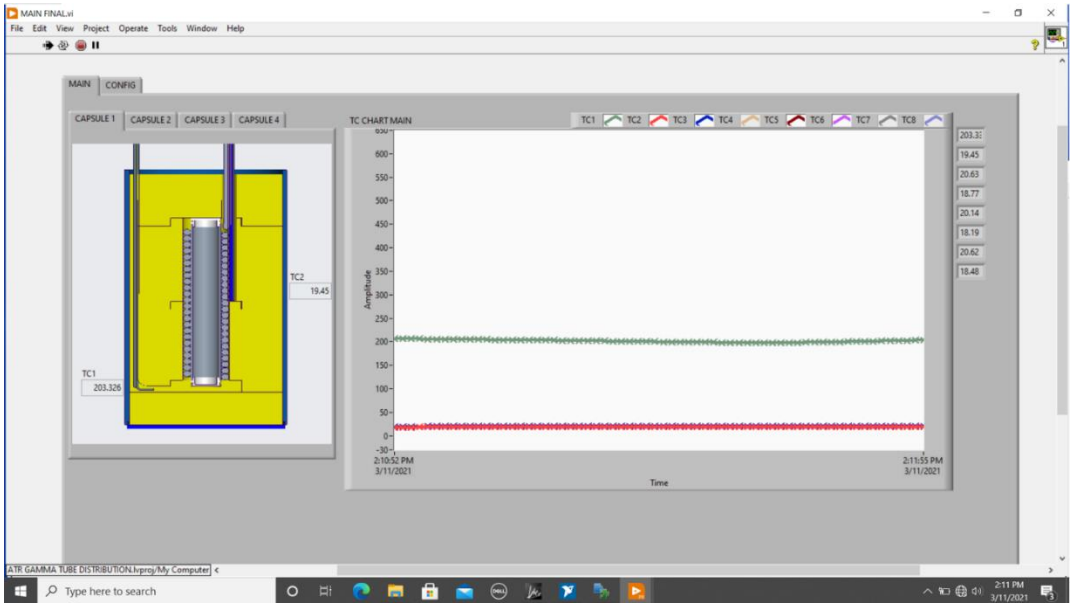

(b)

Figure 10. Photograph of (a) the temperature control and data-logging system in working mode and (b) a temperature control and data-logging screen shot.

Table 2 shows the engraved ID number and test temperature for each salt capsule.

Table 2. Sample ID and test temperature of salt capsules inserted into the ATR gamma tube.

Engraved ID for each salt capsule	Test temperature (°C)
TPRC-01	600
TPRC-02	300
TPRC-03	150
TPRC-04	75 to 131

3.2 Visual observations of the salt capsules after gamma irradiation

Figure 11 shows pictures of the salt capsule assembly immediately after removal from the ATR gamma tube. Some degradation due to the conditions in the gamma tube was observed. The carbon steel rod appears rusted from moisture in the gamma tube, the thermocouple connectors show discoloration from irradiation. The physical impact of the high gamma radiation dose was essentially negligible to the integrity of the capsule assembly and associated instrumentation, other than the ion chamber used for irradiation dose measurement. The ion chamber was the only component that suffered significant degradation from the high gamma field. Figure 12 shows the four salt capsules after disassembly. The health physics technicians (HPT) surveyed all the salt capsules and all other components that were loaded into the ATR gamma tube. No radioactive contamination was observed during the survey process, clearly showing the sealing of the capsules was not broken during the more than 3-month gramma irradiation.

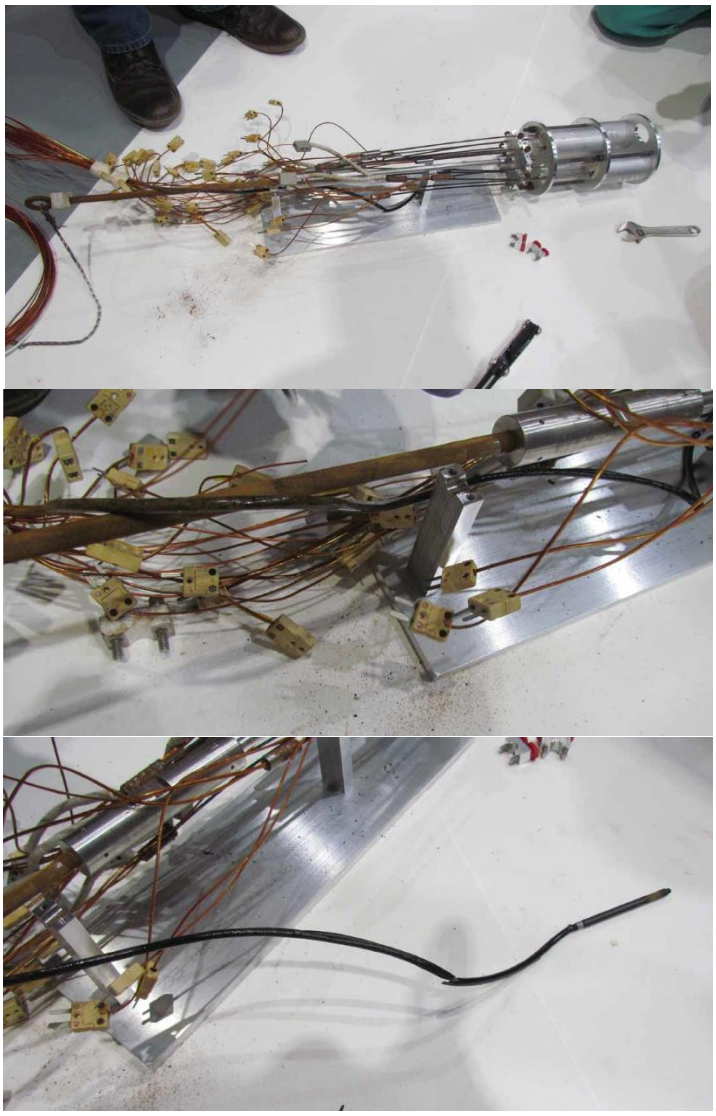

Figure 11. Photographs of the salt assembly immediately after removal from the ATR gamma tube.

Figure 12. Photograph of the NaCl-UCl_3 salt capsules after disassembly.

Figure 13. HPT surveying the salt capsules and other capsule assembly components.

3.3 Temperature Profiles

Temperature data for each thermocouple was recorded once per second over the course of the experiment and logged in daily reported files on the computer. To compile the data, each data file was parsed to one-minute intervals to reduce the data to a using a custom Excel macro and then compiled into a single spreadsheet. The compiled temperature profiles for the control and limit thermocouples the four capsules over the course of the experiment are shown in Figure 14. It should be noted that the control thermocouple was in direct contact with the capsule bottom, while the limit thermocouple was in contact with the outer diameter of the heater, as shown in the capsule cross section in Figure 10. The difference in location resulted in the temperature differences shown in Figure 14 between the control and limit thermocouples. The experimental temperatures for each capsule are assumed to be those of the control thermocouples, as they were in direct contact with the capsule. The thickness of the horizontal lines is a result of oscillations in temperature due to the PID controller operation and represents the high and low temperature bands for the experiment. The gap in data between June 9th and June 15th is a result of the computer malfunction noted above. The temperature control of the experiment was not impacted by the interruption of data collection.

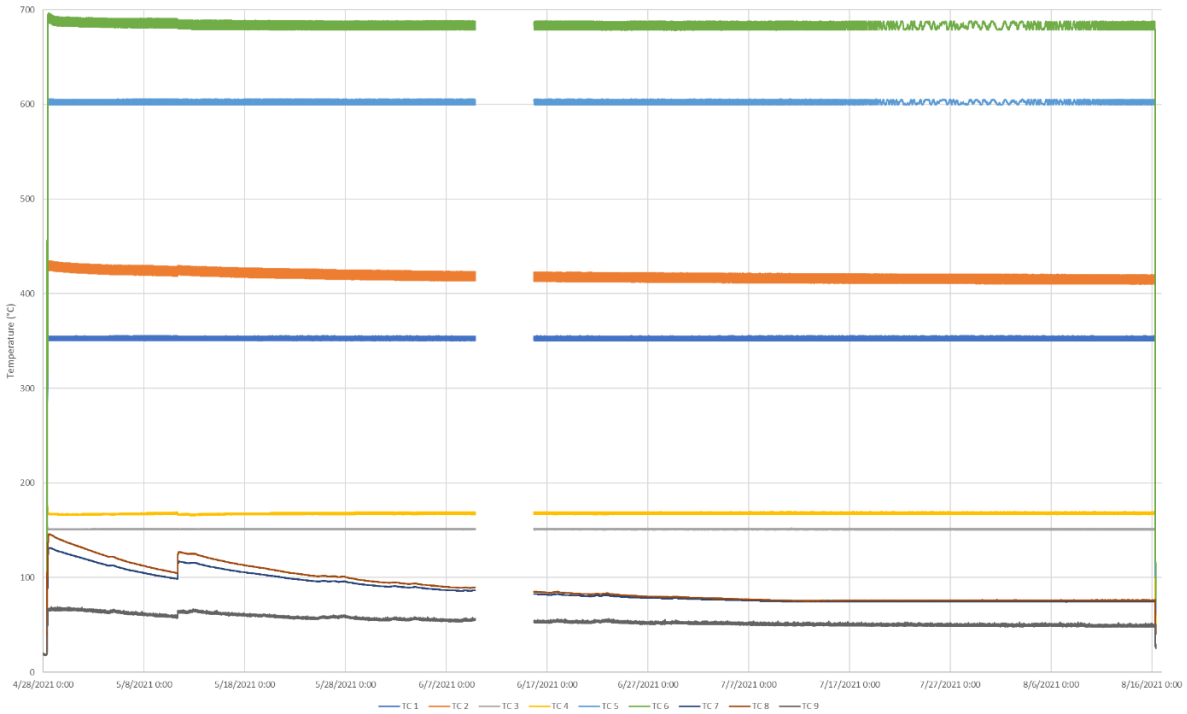

Figure 14. Temperature profiles for the four capsules over the course of the experiment. TC 1 and TC 2 correspond to capsule 2 control and limit thermocouples, respectively, TC 3 and TC 4 correspond to Capsule 3 control and limit thermocouples, respectively, TC 5 and TC 6 correspond to Capsule 1 control and limit thermocouples, respectively, and TC 7 and TC 8 correspond to Capsule 4 control and limit thermocouples, respectively. TC 9 recorded the ambient temperature inside the gamma tube at the experiment location. The increase in temperature for Capsule 4 on May 11th corresponds to the fuel movement on that date.

Interestingly, the decay of the fuel and decrease in dose rate can be observed in the temperature profile for Capsule 4. While the temperature set point for this experiment was 75°C, gamma heating and the insulation around the capsule were sufficient to maintain elevated temperatures above the set point for much of the duration of the experiment. The maximum temperature of 131°C for this capsule was reached within 4 hours after the start of the experiment. A sike in temperature was also recorded on May 11th corresponding to the fuel movement. The dose rate had decreased to the point that the heater was required to maintain the 75°C setpoint for Capsule 4 by mid-July.

3.4 Dose and Dose Rate during Gamma Irradiation

The dose over time was recorded from experiment insertion on April 28 to June 15, 2021. The high total absorbed dose, along with the continuously high dose rates, degraded the performance of the ion chamber used for these measurements. Consequently, the recorded data became less reliable over time, particularly after the fuel was rearranged on May 11th to increase the dose rate. Data after June 15th showed erratic values, fluctuating from positive values above the initial dose rate, to negative dose rates, indicating failure of the ion chamber. This data is omitted from the report for clarity. Consequently, the dose rate data was fit with an exponential function to estimate the true total absorbed dose. The measured and modeled dose rates and the total absorbed dose as functions of time for the irradiation experiment are shown in Figure 15.

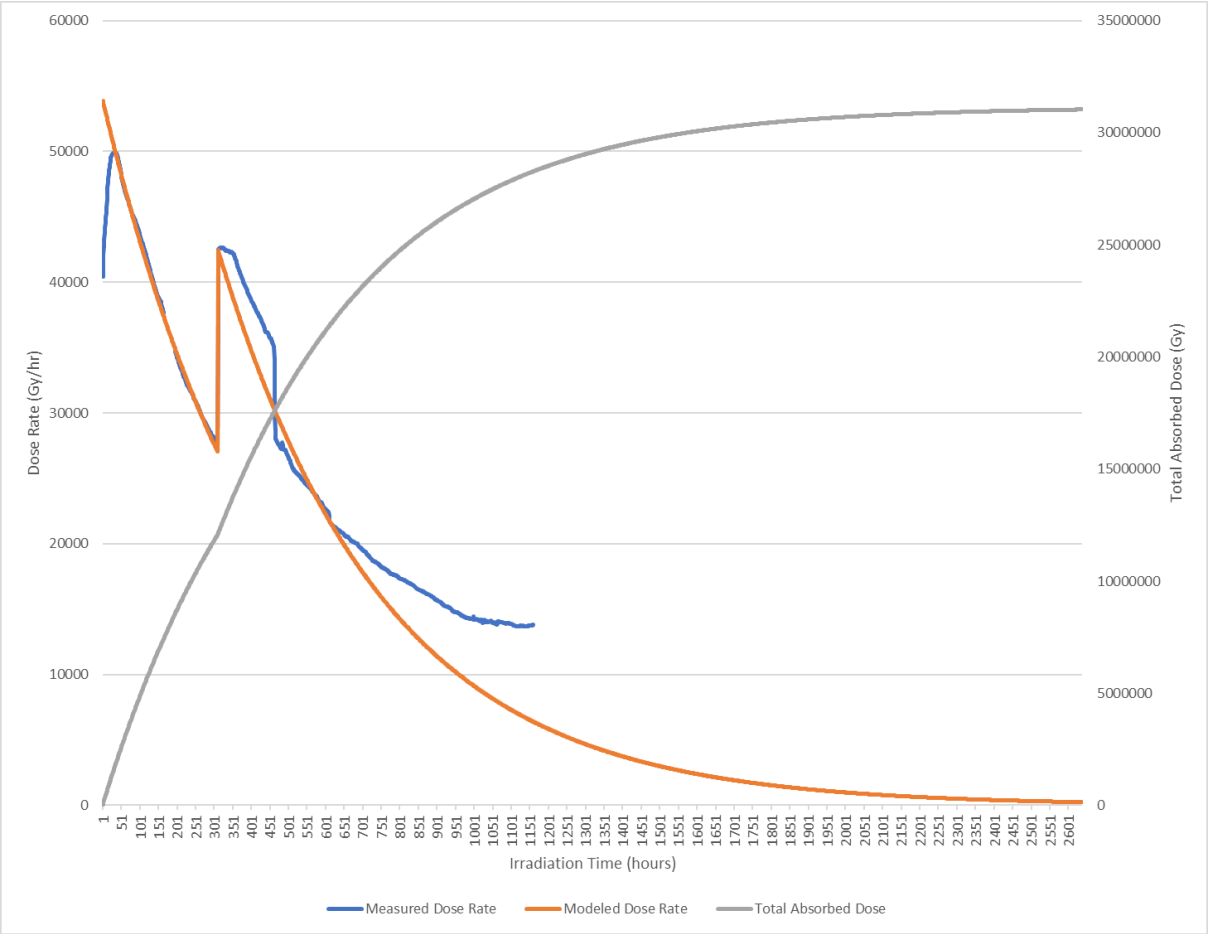

Figure 15. Measured and modeled dose rate recorded during the gamma irradiation experiment. The increase in dose rate as a result of the fuel movement on May 11th can be observed at 310 hr. The ion chamber reliability began to degrade after May 16th, as can be observed by the large unexplained decrease in measured dose rate at approximately 460hr, the noise in the subsequent data, and the plateau of the dose rate at approximately 13000 Gy/hr. The increase in measured dose rate at the beginning of the experiment does not have any known cause. Data after June 15th is considered unusable due to the failure of the electrometer and ion chamber, as noted in text.

For this model, the period from April 30th through May 11th ($t = 0\ to\ t_m = 310\ hr$) was used to determine the exponential decay term, λ, and the dose rate, R_1 at theoretical $t = 0$ for period 1. The same exponential decay term was used for the second period, after the fuel movement occurred, while the intercept for this period was set such that the decay curve intercepts the measured dose rate at $t = t_{m+1}$. Integration of the resulting curve gives the total absorbed dose for the experiment. This model is summarized below.

$$Dose\ (Gy) = \int_0^{t_m} R_1 e^{\lambda t} dt + \int_{t_{m+1}}^{t_f} R_2 e^{\lambda t}$$

$$R_1 = 54{,}000\ Gy/hour$$
$$R_2 = 85{,}000\ Gy/hour$$
$$\lambda = -0.00223011\ hour^{-1}$$
$$t_m = 310\ hours$$

$$t_f = 2638\ hours$$

$$Dose\ (Gy) = 3.1x10^7 Gy$$

From this calculation, the total absorbed dose is estimated to be approximately 31 MGy.

3.5 GASR Analysis Results

Following irradiation, the capsules were transferred from ATR back to MFC for analysis and storage. The four salt samples were then analyzed in the GASR instrument in HFEF. The pressure and volume inside the salt capsules were calculated from the expanded pressure measurements in GASR.

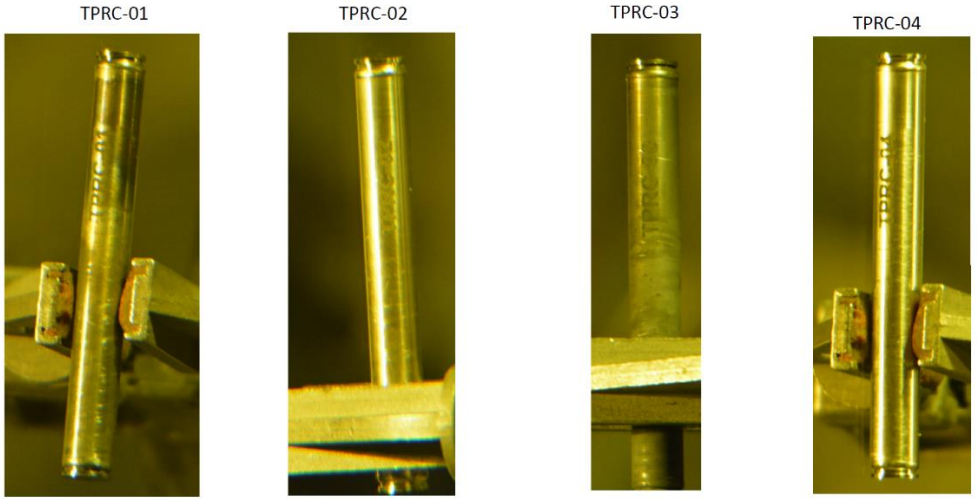

(a)

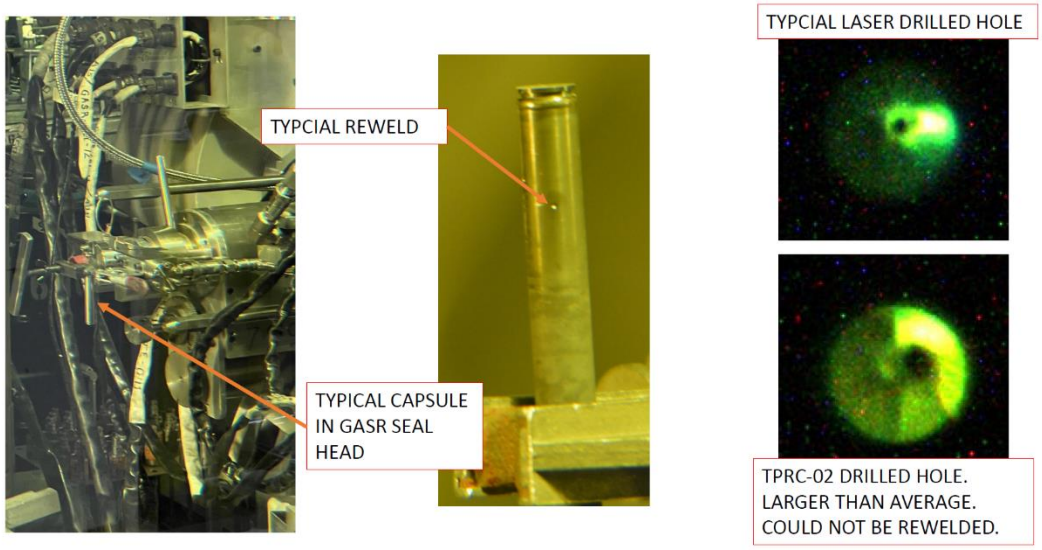

(b)

Figure 16. Photographs of four salt capsules before GASR analysis and the typical process for GASR analysis.

Figure 17 shows the gas pressure analyzed by the GASR instrument. The baseline pressure is from measurements of three capsules which contained aluminum rods of similar size to the salt samples. The uncertainty is 2.6 psi. For the salt capsules, the The gas pressure in each capsule is in the range of 10.9 to 11.9 psia. This range indicates that the pressure in the capsules matched the slightly negative pressure of the AFCI glovebox within which the capsules were fabricated. No indication of significant radiolysis was observed.

It was expected that some chlorine gas would be formed due to gamma radiolysis in the NaCl-UCl_3 salt at 75°C and 175°C, but the amount of the gas formed under the ATR gamma tube radiation conditions is insignificant and is below the detection limit of the GASR instrument in HFEF.

The gas volume analyzed by GASR in the capsules after radiolysis is shown in Figure 18. The gas volume in the salt capsules is in the range of 2.37 to 2.45 cc, with a measurement error of 0.01 to 0.1 cc. The volume measurements met expectations based on the size of the salt pellets that were loaded into the capsules. The full GASR data results are shown in Appendix B.

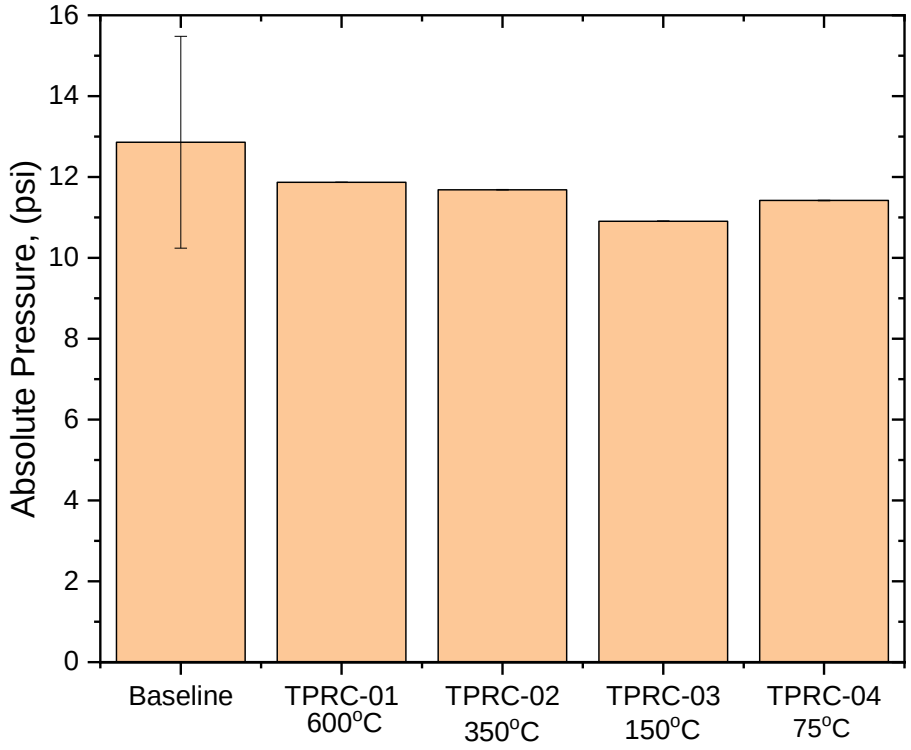

Figure 17. Pressure of salt capsules analyzed by GASR.

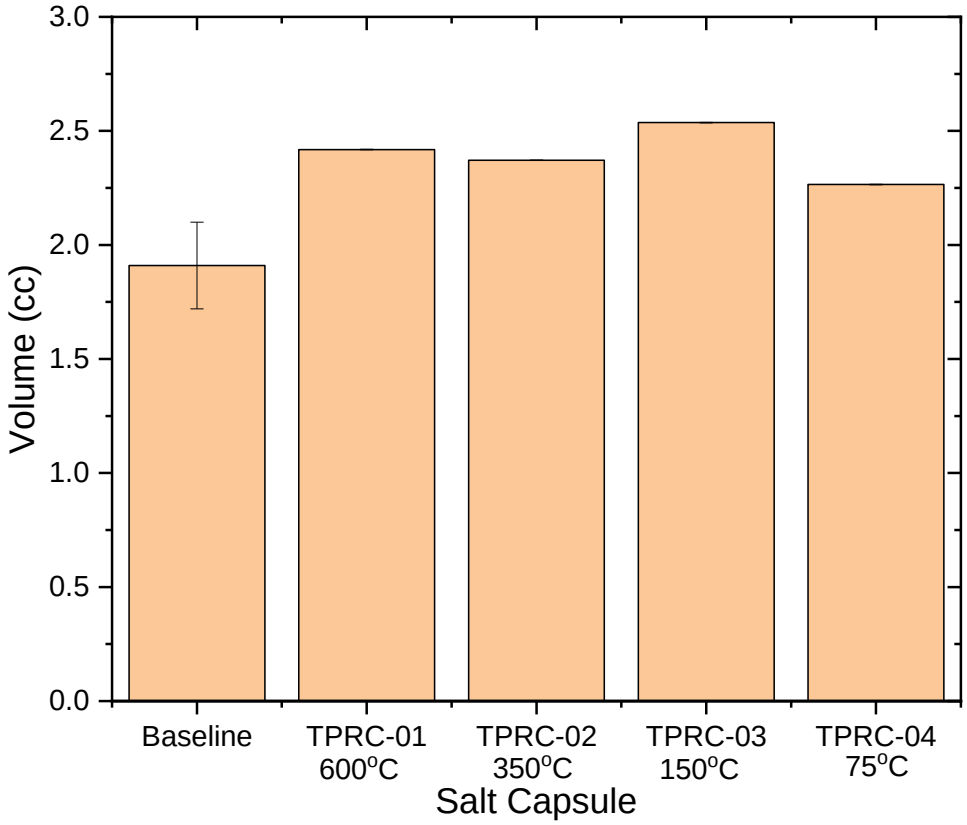

Figure 18. Gas volume of salt capsules analyzed by GASR

For each capsule, after drilling the capsule open with the laser and completion of the first pressure measurement, the capsules were then re-pressurized with approximately 15 psia of helium gas. The laser was de-focused, and a welding operation attempted. Welding the capsules closed with helium was successful on all capsules except TPRC-02 whose initial drilled hole was too large to re-weld. The successfully welded capsules were then re-drilled an additional pressure measurement taken. The reason for performing these additional operations was to gain more experience and data with the newly installed GASR replacement system. The pressure measurements on the backfilled helium are not directly related to the radiolysis investigation but do provide confidence that the newly installed GASR system was performing as expected.

3.6 Direct Chlorine Detection

Extensive efforts were made as part of this study to develop a means to directly measure chlorine gas concentration that was expected to be generated within the capsules at low concentrations due to radiolysis. The original experimental plan was to collect gas samples from the capsules using GASR and to ship the gas samples to the MFC analytical laboratory for measurement of chlorine concentration.

The first effort at developing a means to measure chlorine concentration was to utilize common industrial electrochemical cell sensors because they are widespread and have the ability to measure chlorine at very low concentrations for personnel safety. When working with sales engineers it was realized that these detectors would not be able to detect small volumes of chlorine in a background of argon gas. This type of electrochemical cell requires a substantial volume of gas as well as a background of air, due to the necessity of moisture and oxygen for the half-cell reactions that detect chlorine.

Chlorine specific colorimetric sampling tubes (Drager tubes) were also investigated, due to their ability to detect small quantities of Cl_2 independent of the matrix gas composition. Unfortunately, performing measurements using this method of gas sampling system requires a relatively large volume of gas at atmospheric pressure and specific flow rate, using a manufacturer specified and calibrated pump for the calibration of the tube to be valid. The bellows-type pumps used for these tubes cannot be plumbed into a fixed volume container easily, which would necessitate opening the capsules inside of a glovebag containing the pump and colorimetric tube. Assuming a glovebag volume of 30 liters and capsule headspace volume of 2cc, this would result in a dilution factor on the order of 15,000. The most sensitive available Draeger tube has a detection threshold of 0.2ppm, resulting in a lower detection threshold for this experiment of approximately 3000ppm. Consequently, due to the small gas volume present in the capsules, the gas sample would have to be diluted to the point that the expected concentration (<1000ppm) would be below the detection limit of the tubes and would introduce a significant amount of error in the measurement as well as experimental difficulty and complexity.

Gas mass spectroscopy (GMS) was also major effort made in this regard, due to the low theoretical detection limits, high precision, and low sample pressure/volume requirements. A series of low concentration standards in lecture bottles (maximum 100ppm Cl_2 in an Ar matrix) were purchased to attempt to make measurements with a GMS located at MFC's analytical laboratory. Despite significant efforts to troubleshoot the system, Cl_2 could not be detected using this technique. The hypothesis is that due to the reactivity of Cl_2 and the complexity of the gas manifold, low concentration of Cl_2 and the sample introduction system on the instrument itself, it is likely that the Cl_2 quantitatively reacted and/or adsorbed with/into the materials in the system prior to its introduction to the instrument. All components of the gas manifold and sample introduction system were evaluated for compatibility with Cl_2 gas and several were replaced; however, the highly reactive chlorine gas could not be detected at a low enough concentration to warrant further efforts.

A UV spectrometer specifically designed for chlorine detection was also explored at the MFC analytical laboratory. The custom spectrometry system shown in Figure 19 was developed in collaboration with Port City Instruments and Pike Technologies. The system consisted of a custom stainless steel White cell with an optical path length of 5 meters and a cell volume of 1 liter. Use of a multi-pass cell allows for increased optical path length and consequently increased detection sensitivity for rarified gasses when using optical absorption spectroscopy. However, these types of cells are typically optimized for IR wavelengths due to FTIR spectroscopy being the dominant gas-phase optical detection technique for other applications. Due to the diatomic nature of chlorine, it is not optically active in the IR region, and only possesses a single absorption band at 325nm. Consequently, the optical design of the system had to be tailored for the detection of chlorine. Pike Technologies provided the White cell, while design of the light source, detection system, software, and coupling of the White cell to the system were performed by Port City Instruments. More details on the UV gas spectrometer are given in the operating manual, copied in Appendix C.

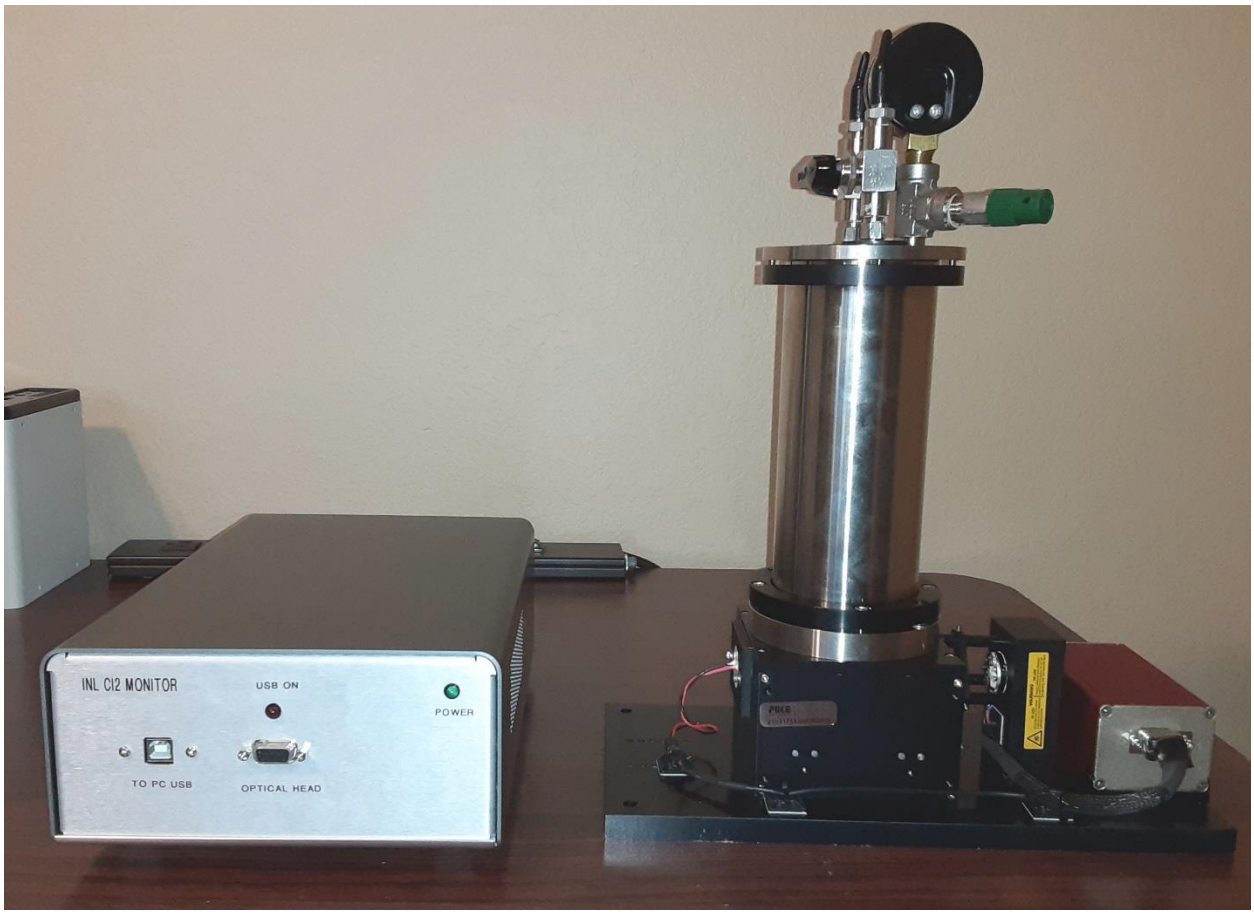

Figure 19: Custom Port City Instruments UV spectrometer for detection of Cl_2 gas at low concentrations.

After several tests utilizing the same standards used with the GMS, this system too yielded detection limits that were too high for use with the small volumes, low pressure, and low concentrations expected in the capsules. The 100ppm Cl_2 standard was found to be detectable, however, only at pressures approximately 10x the expected sample pressure following collection using GASR, expansion into the sample container, and subsequent expansion into the spectrometer, implying a lower detection threshold of 1000ppm. Additionally, the signal quickly decayed following introduction of the Cl_2 standard into the system, indicating that the sample was reacting with the White cell, making validation of the measurement impossible.

From the combined experience working with the Cl_2 gas standards, it was expected that any Cl_2 gas samples collected in GASR from the radiolysis capsules would quickly react with the gas manifold in GASR and the sampling container, before measurement in the MFC AL could be performed. When combined with the high detection threshold and sample lifetime in the spectrometer, confident detection of any Cl_2 in the gas sample was deemed to be extremely unlikely. Coupling the UV spectrometer directly to the GASR sampling manifold, while theoretically possible, was determined to involve a significant amount of engineering effort that was beyond the scope of this project. Consequently, direct detection of chlorine concentration was thus abandoned due to project constraints, and pressure measurements via GASR were utilized for indication of the presence of radiolytically generated gas in the capsules.

3.7 Future Work

Due to budget and schedule restrictions, no analyses beyond GASR pressure measurements have been performed to date. To further elucidate the effects of gamma irradiation on the salt capsules, several techniques could be employed. Due to the reactivity of chlorine gas and the temperatures involved in this experiment, it is possible that radiolytically generated chlorine gas that was released from the salt crystal structure may have reacted directly with the capsule walls to form metal chlorides. Scanning electron microscopy equipped with energy dispersive X-ray spectroscopy could be used to determine the microstructure and composition changes of the surface of the capsule wall, and therefore estimate the rate of chlorine gas generation. In the case of the capsule held in the liquid state, the effects of radiation assisted corrosion in molten NaCl-UCl_3 could also be observed.

To observe the effects of radiation on the salt itself, we suggest using differential scanning calorimetry to detect phase transformations indicative of annealing, defect recombination, or other processes that differ from the baseline, unirradiated salt. Additionally, electron paramagnetic resonance (EPR) should be used to study the defect structure in the irradiated salt samples. EPR is useful for determining the nature of unpaired electrons and defect structure in irradiated materials, and has recently been applied to other salt systems by the Molten Salts in Extreme Environments (MSEE) Energy Frontiers Research Center (EFRC).

4. Summary

This report documents the results of the gamma ray irradiation of NaCl-UCl_3 eutectic salt in the gamma tube at the advanced test reactor spent fuel pool, and analysis of capsules by the gas sample assay and recharge system. NaCl-UCl_3 salt capsules were irradiated at temperatures of 75°C-131°C, 150°C, 300°C and 600°C shortly after the CIC of the ATR in April of 2021, for a duration of 2638 hours. The ATR gamma radiolysis test was completed successfully. Based on the GASR analysis results, the quantity of Cl_2 gas released from NaCl-UCl_3 under the test conditions was non-detectable, and therefore, it is likely that releases of Cl_2 gas during long term storage of used MCFR fuel under similar conditions will be insignificant. To further elucidate the radiolysis effect on the NaCl-UCl_3 salts and reach a more definitive conclusion, advanced analyses such as SEM-EDS, EPR, and DSC are recommended to analyze the capsule wall and salt samples.

5. References

1. Levy, P. W., Loman, J. M. & Kierstead, J. A. Radiation induced F-center and colloid formation in synthetic NaCl and natural rock salt: Applications to radioactive waste repositories. *Nucl. Instruments Methods Phys. Res. Sect. B Beam Interact. with Mater. Atoms* **1**, 549–556 (1984).
2. Levy, P. W. Radiation damage studies on non-metals utilizing measurements made during irradiation. *J. Phys. Chem. Solids* **52**, 319–349 (1991).
3. Soppe, W. J. & Prij, J. Kinetic model calculations of colloid growth in NaCl. *Nucl. Instruments Methods Phys. Res. Sect. B Beam Interact. with Mater. Atoms* **91**, 92–96 (1994).
4. Levy, P. W. Overview Of Nuclear Radiation Damage Processes: Phenomenological Features Of Radiation Damage In Crystals And Glasses. in *Radiation Effects on Optical Materials* (ed. Levy, P. W.) **0541**, 2 (1985).
5. Akram, N., Blanchard, J. C., Gaudez, M. T. & Toulhoat, P. Compared Study of Radiolysis-Induced Gas Liberation in Rocksalt from Various Origins. *MRS Proc.* **294**, 447 (1992).
6. Bergsma, J., Helmholdt, R. B. & Heijboer, R. J. Radiation dose deposition and colloid formation

in a rock salt waste repository. *Nucl. Technol.* **71**, 597–616 (1985).

7. Boizot, B. *et al.* Migration and segregation of sodium under β-irradiation in nuclear glasses. *Nucl. Instruments Methods Phys. Res. Sect. B Beam Interact. with Mater. Atoms* **166**–**167**, 500–504 (2000).

8. Cubicciotti, D. & Davies, J. H. The release of iodine from iodide salts by gamma radiolysis. *Nucl. Sci. Eng.* **60**, 314–319 (1976).

9. Makarov, I. E., Zhukova, T. N., Pikaev, A. K. & Spitsyn, V. I. Oxidizing agents produced by radiolysis of alkali-metal halide melts. *Bull. Acad. Sci. USSR Div. Chem. Sci.* **31**, 662–666 (1982).

10. Tandon, L. Radiolysis of Salts and Long-Term Storage Materials in Plutonium Storage Containers. *Los Alamos Natl. Lab.* **LA-13725-M**, 1–87 (2000).

11. Soppe, W. J., Donker, H., García Celma, A. & Prij, J. Radiation-induced stored energy in rock salt. *J. Nucl. Mater.* **217**, 1–31 (1994).

12. Del Cul, G. D., Icenhour, A. S. & Simmons, D. W. Prototype Tests for the Recovery and Conversion of UF6 Chemisorbed in NaF Traps for the Molten Salt Reactor Remediation Project. **5450**, 35 (2000).

13. Forsberg, C. W. Molten-Salt-Reactor Technology Gaps. *Proc. ICAPP '06* (2006).

14. Grimes, W. R. Radiation chemistry of MSR system. (1963).

15. Haubenreich, P. N. Fluorine production and recombination in frozen MSR salts after reactor operation. (1970).

16. Peretz, F. J., Rushton, J. E., Faulkner, R. L., Walker, K. L. & Del Cul, G. D. Removal of Uranium and Salt from the Molten Salt Reactor Experiment. *ORNL/CP-98146* (1998).

17. Toth, L. M. & Felker, L. K. Fluorine generation by gamma radiolysis of a fluoride salt mixture. *Radiat. Eff. Defects Solids* **112**, 201–210 (1990).

18. Diamond, D. J., Brown, N. R., Denning, R. & Bajorek, S. Phenomena Important in Molten Salt Reactor Simulations. *Brookhaven Natl. Lab.* 1–85 (2018).

6. Appendix A: Engineering Analysis and Calculation Report*

6.1 Scope and Brief Description

The chloride salt, NaCl-$PuCl_3$, is currently being evaluated as a candidate fuel salt for the TerraPower Molten Chloride Fast Reactor (MCFR). However, the radiolytic stability of NaCl-$PuCl_3$ has not been extensively tested within intense radiation environments of fast reactors such as the MCFR. To further understand the radiolysis behavior of NaCl-$PuCl_3$ salt, an experiment in the Advanced Test Reactor (ATR) gamma tube is currently planned to occur during the ATR core internal change-out (CIC) starting in March 2021. This Engineering Calculations and Analysis (ECAR) summarizes the conjugate heat transfer model that was developed of the experiment to demonstrate that the experiment's target temperatures cause only negligible increases in the temperatures of the ATR gamma tube components.

6.2 Design or Technical Parameter Input and Sources

Details of the experiment were acquired from the unreleased document "Design and Experimental Test Plan for Gamma Irradiation of NaCl-PuCl3 Salt for Molten Chloride Fast Reactor".

1) The experiment assembly contains four capsules that are electrically heated. Two cases were explored in this analysis:

    a. The "Target Temperature Case" where the four capsules are heated to: 600°C, 350°C, 150°C, and 75°C, respectively.

    b. The "High Temperature Case" where all four capsules are heated to 800°C.

2) The material properties utilized in the model are detailed in Appendix A.

6.3 Results of Literature Searches and Other Background Data

1) The model geometry of the experiment assembly was provided by the design engineer in a 3D-CAD model (STEP file) through email correspondence. The original file will be included in the Data Files directory of this ECAR.

2) The geometry for the gamma tube and the fuel storage rack were derived from INL drawings 419611 and 117015.

6.4 Assumptions

1) The ATR canal water is assumed to be 26.67°C (80.0°F) (Hawkes, 2015).

2) For the exterior walls of the gamma tube and the fuel storage rack tube a natural convection heat transfer coefficient is specified with an ambient temperature of 26.67°C (80.0°F).

* This ECAR was performed for NaCl-$PuCl_3$ salt which was originally planned for the gamma irradiation test. But the ECAR results also apply to NaCl-UCl_3 salt.

3) The thin annulus of canal water between the fuel storage rack and the gamma tube is modeled as stagnant water where only conductive heat transfer is considered.

4) Natural convection and radiative heat transfer are modeled in the air within the gamma tube.

5) Perfect thermal contact is assumed between all components and air gaps between components are removed. This increases heat transfer to the gamma tube components and therefore is considered conservative.

6) All components inside the insulation of the inner baskets are assumed to be at a constant temperature.

7) The experiment's temperatures are monitored and controlled with thermocouples and electric heaters; therefore, gamma heating was not considered.

6.5 Computer Code Validation

A. Computer type: INL's HPC system Sawtooth which is a 99,792 core HPE SGI 8600 system that is comprised of 2052 compute nodes. Each node contains 2, 24-core Intel Xeon 8268 2.9 GHz processors with 192 GB of RAM. A set of 10 nodes was used for the simulations.

B. Operating System and Version: CentOS operating system

C. Computer program name and revision: Star-CCM+ 2019.3.1 (14.06.013-R8) (Star-CCM+ 14.06.013-R8, 2019)

D. Evidence of, or reference to, computer program validation: See Appendix B, ECAR-4345 (Appendix C) (Kennedy, 2018), and ECAR-4957 (Appendix A) (Xing, 2020)

E. Bases supporting application of the computer program to the specific physical problem: Star-CCM+ is a computational fluid dynamics (CFD) finite volume (FV) solver that is specifically designed for fluid and thermal analysis. It is also listed in the INL Enterprise Architecture (EA) repository of qualified scientific and engineering analysis software (PLN-3597, Enterprise Engineering/Scientific Software, Rev 6, 2016).

6.6 Discussion/Analysis

6.6.1 Model Geometry

The ATR gamma tube is located in the spent fuel pool of the ATR canal surrounded by ATR fuel elements as shown in Figure 20. The tube is manufactured from 5" schedule 10 SS304 pipe with lead shielding caps at the top and bottom. Overall, it is ~625 cm (20.5 ft) tall and has an inner diameter of ~13.45 cm (5.295").

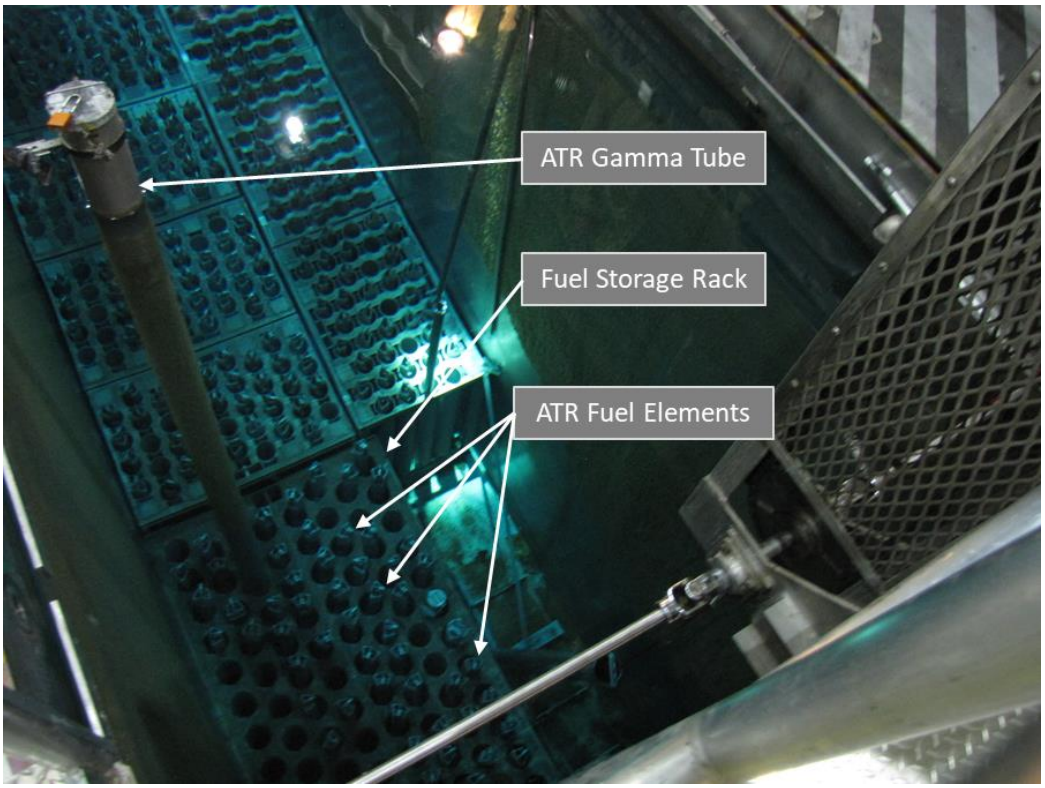

Figure 20. Photo of the ATR gamma tube in the spent fuel pool of the ATR canal.

A step file of the experiment assembly was provided by the experiment's design engineer and is shown in Figure 21. Overall, the assembly is about 84 cm (33") tall and contains 4 inner baskets held in place by the stainless-steel outer basket and will be lowered into the gamma tube using the lifting ring at the top. Each stainless-steel inner basket contains insulation comprised of WDS-Shape, a 250W electric heater wrapped around an Inconel 625 capsule, and two thermocouples for monitoring and controlling the capsule temperature. A salt sample (not shown in Figure 21) is added to each of the four Inconel 625 capsules which will be heated during the experiment to the temperatures detailed in Table 3 (Target Temperature Case). The hotter two inner baskets are placed at the top position (labeled 1 and 2 in Figure 21) and the cooler inner baskets are at the bottom position (labeled 3 and 4 in Figure 21). In the High Temperature Case all four capsules will be heated to 800°C, which was selected based on the absence of properties for WDS-Shape at temperatures >800°C (Morgan Advanced Materials, 2019).

Table 3. Target temperatures of the NaCl-$PuCl_3$ salt samples.

Inner Basket ID	Target Temperature (°C)
1	600
2	350
3	150
4	75

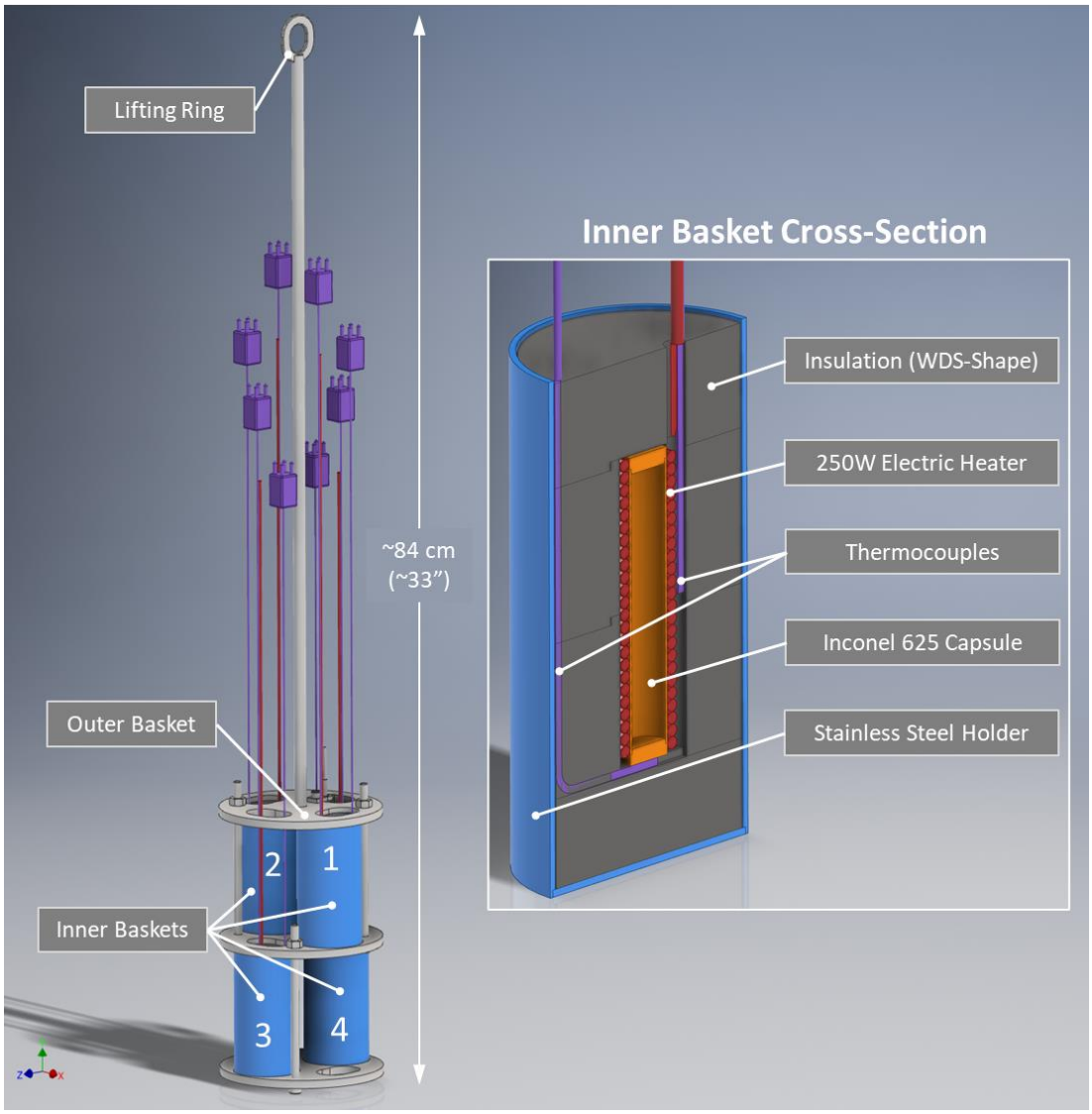

Figure 21. 3D-CAD geometry of the experiment assembly with a cross section of an inner basket.

The model geometry imported to Star-CCM+ is shown in Figure 22. It contains the gamma tube (derived from DWG-419611), an Al6061 fuel storage rack tube (derived from DWG-117015), a stagnant water annulus between the gamma tube and the storage rack tube, the simplified experiment assembly, and the air inside the gamma tube where natural convection occurs. The experiment assembly was simplified by combining the five separate parts that comprise the insulation into one part and removing the electric heaters, thermocouples, and capsules from the inside of the inner basket's insulation.

With the components inside the inner baskets removed, a constant temperature is prescribed on the inside surfaces of the insulation. This implicitly assumes that everything in this cavity is at the prescribed target temperature. The outside surfaces of the gamma tube and storage rack tube were prescribed with a heat transfer coefficient as calculated in Appendix A.

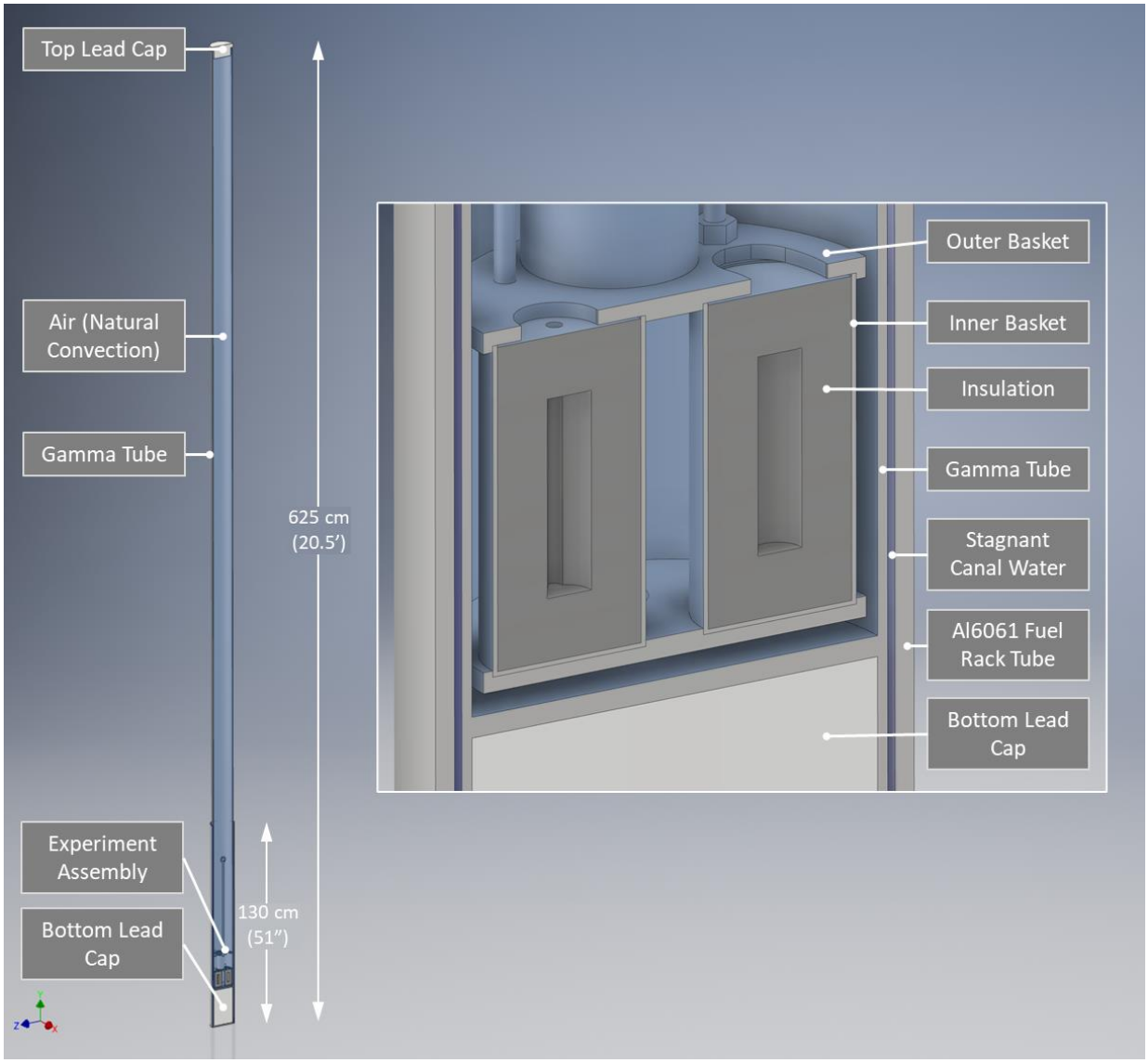

Figure 22. Star-CCM+ model geometry of the simplified experiment assembly in the gamma tube.

Polyhedral cells were utilized to discretize the geometry shown in Figure 22. Three meshes were created in Star-CCM+ and cross sections of these meshes zoomed in to the area near the experiment's inner baskets are shown in Figure 23. The fine, finer, and finest meshes that were tested have 8.24, 13.4, and 23.4 million cells, respectively. To compare the meshes, the maximum temperature of the gamma tube as the model converged to a quasi-steady state using each mesh is shown in Figure 24. Overall, all three meshes exhibit very similar results therefore the solution can be considered mesh independent. For all subsequent results presented herein the finest mesh was utilized.

The air inside the gamma tube was modeled as an ideal gas and gravity was accounted for in the -y direction thereby inducing natural convection to occur in the air. The flowing air was modeled using the Reynolds-Averaged-Navier-Stokes (RANS) SST k-Omega turbulence model with the "all y+ wall

treatment" model. To accurately capture the turbulent boundary layer, a prism layer mesh was added to the mesh of the air to add mesh refinement near the walls. This near-wall mesh refinement yielded wall y+ values (nondimensional distance from the wall) shown in Figure 25. Ideally, wall y+ values should be less than unity in order to accurately capture the fluid solution in the viscous sublayer of the boundary layer. All walls were assumed to be no-slip and smooth.

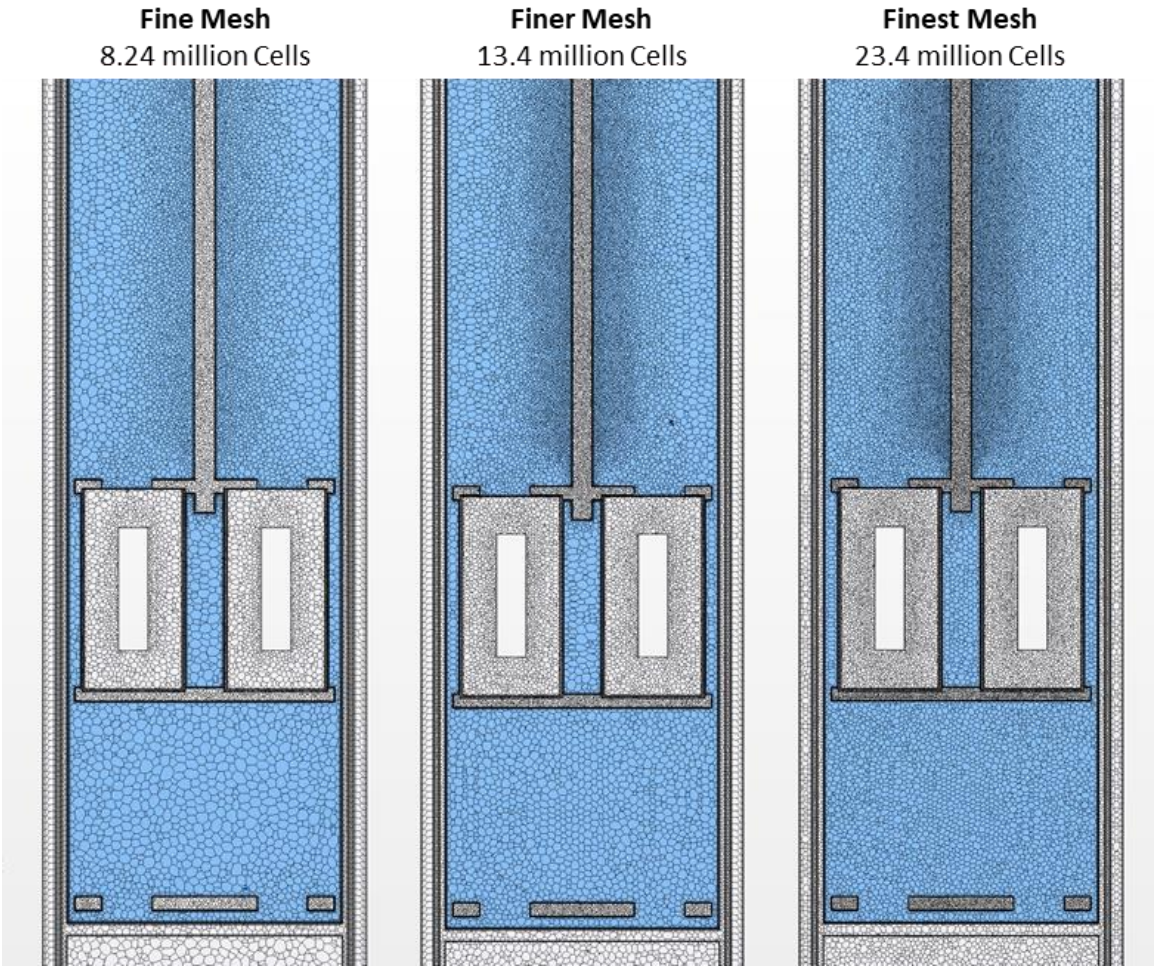

Figure 23. Cross sections of the three polyhedral meshes of the experiment geometry utilized to verify mesh independence in Star-CCM+. Solid parts are white and the air in the gamma tube is blue.

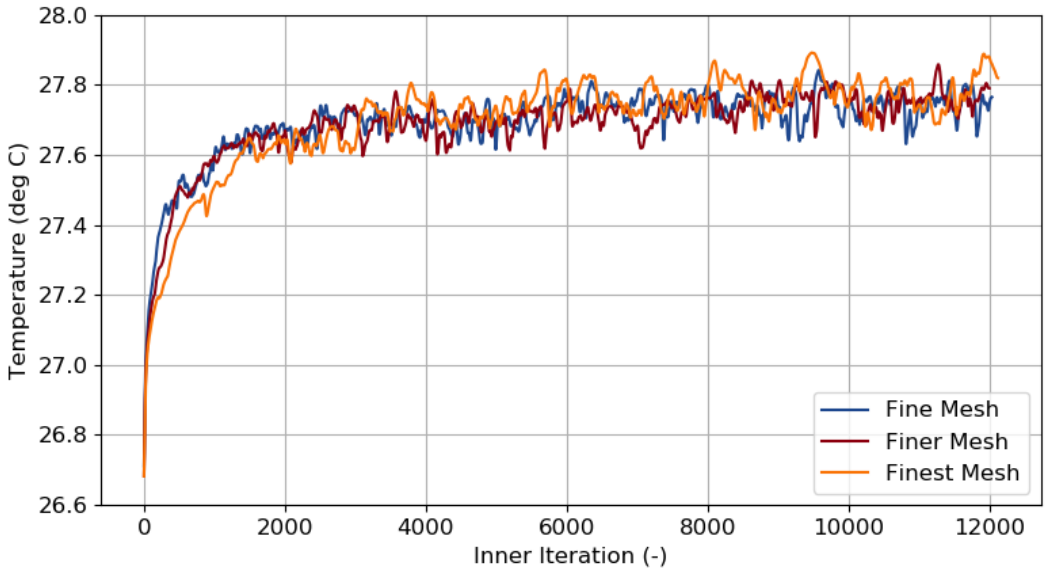

Figure 24. Maximum temperature of the gamma tube vs solver iterations for three different mesh sizes.

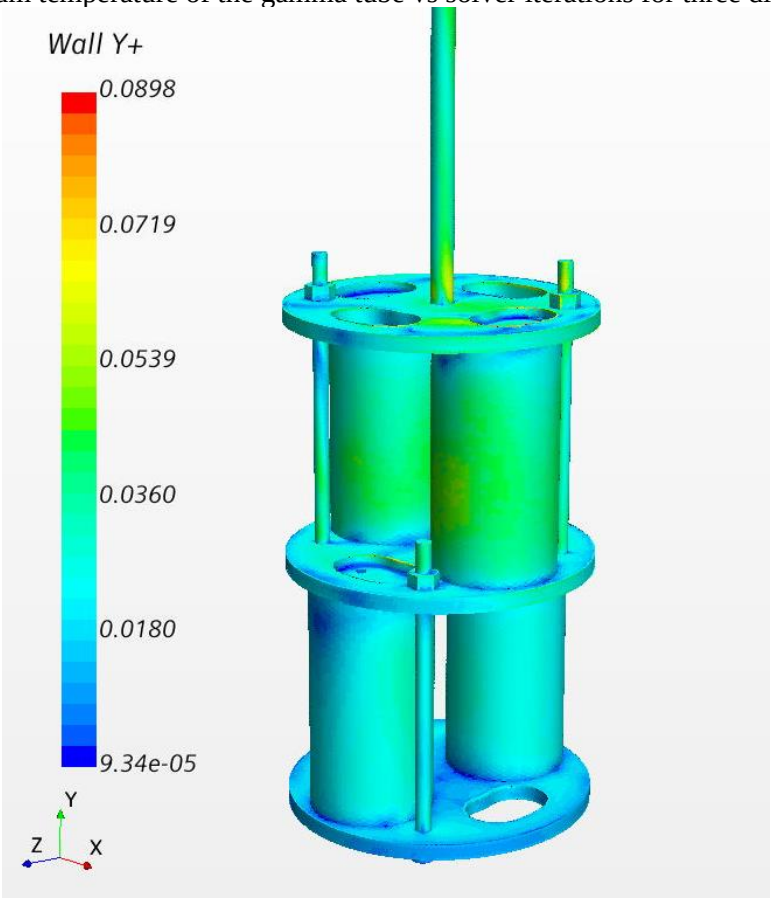

Figure 25. Wall y+ values on the surfaces of the experiment assembly using the finest mesh.

6.7 Model Results

6.7.1 Target Experiment Temperature Case

As described in the analysis request in Appendix C the temperatures of the gamma tube components are of greatest interest to the authors of the experiment safety analysis (ESA). The temperatures of the top and bottom lead caps are shown in Figure 26 for the target temperature case. The maximum temperature of 26.9°C occurs in the bottom lead cap which is only ~0.2°C higher than the assumed water temperature of the canal (26.7°C). Figure 27 shows the temperature of the interior wall of the gamma tube with a zoomed view near the experiment assembly. The maximum temperature of the gamma tube is about 27.8°C and as expected occurs near the hottest inner basket. While the gamma tube's temperature is higher than the lead caps, it is still only ~1.2°C warmer than the canal's water temperature (26.7°C).

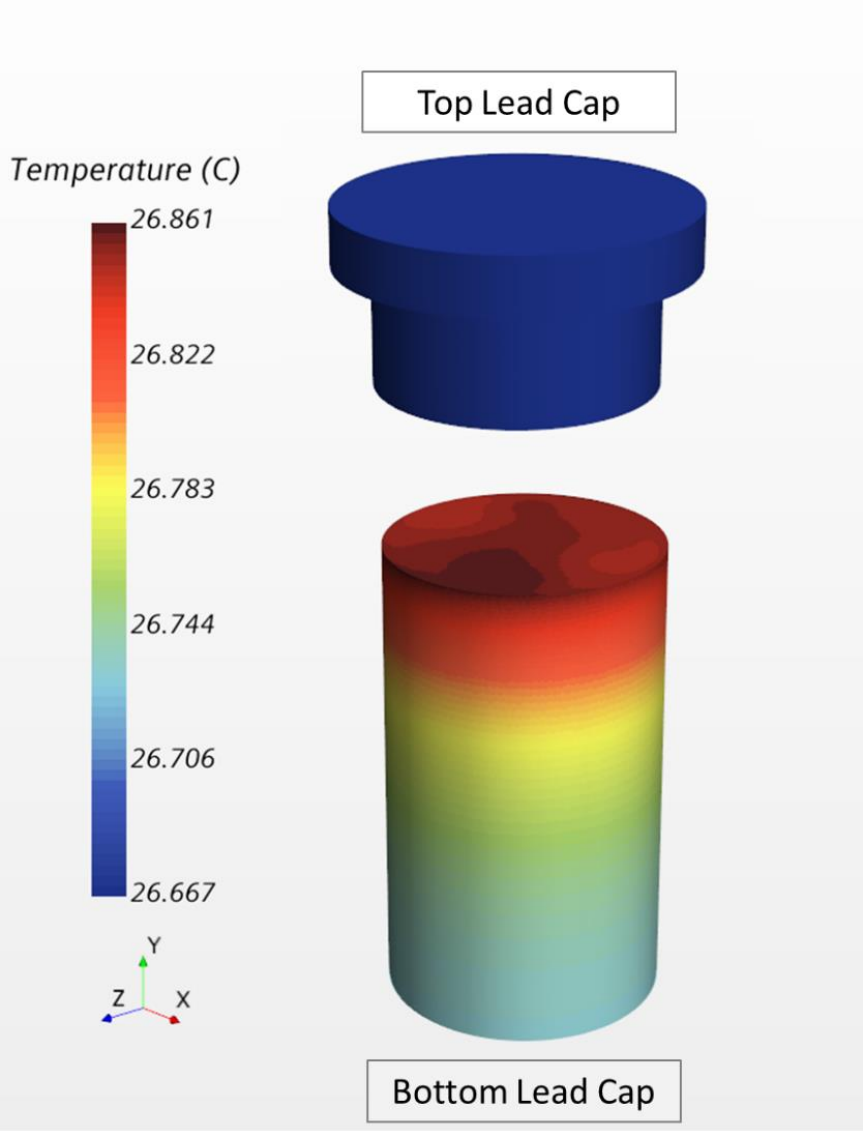

Figure 26. Target Temperature Case – temperature of the top and bottom lead caps.

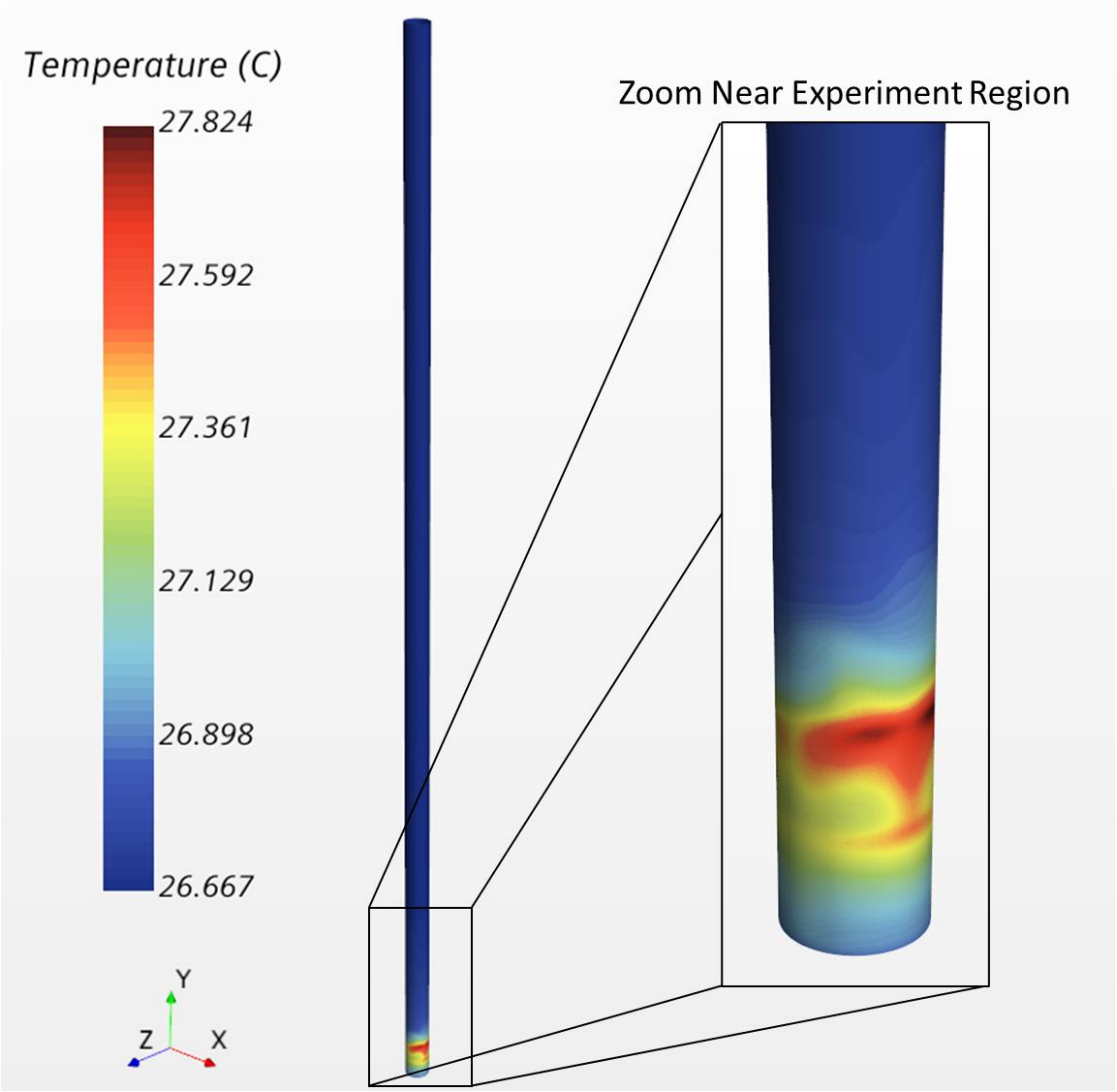

Figure 27. Target Temperature Case – temperature of the gamma tube's internal walls with zoomed view near the experiment.

The temperature of the air above the inner baskets is also of interest for sizing the protection/sheathing of the heater/thermocouple leads. In Figure 28 the temperature of the air inside the gamma tube is shown. Cross sections through the top (XY) and bottom (YZ) sets of inner baskets are shown on the left and right, respectively. As expected, the highest temperature (64.8°C) is around the wall of the hottest inner basket however overall, the temperatures are only about 30 to 40°C in the bulk of the air volume around the inner baskets. It should be noted that the temperature magnitudes/contours shown in Figure 26 through Figure 28 fluctuate slightly as the simulation iterates due to the unsteady nature of the air circulating in the gamma tube.

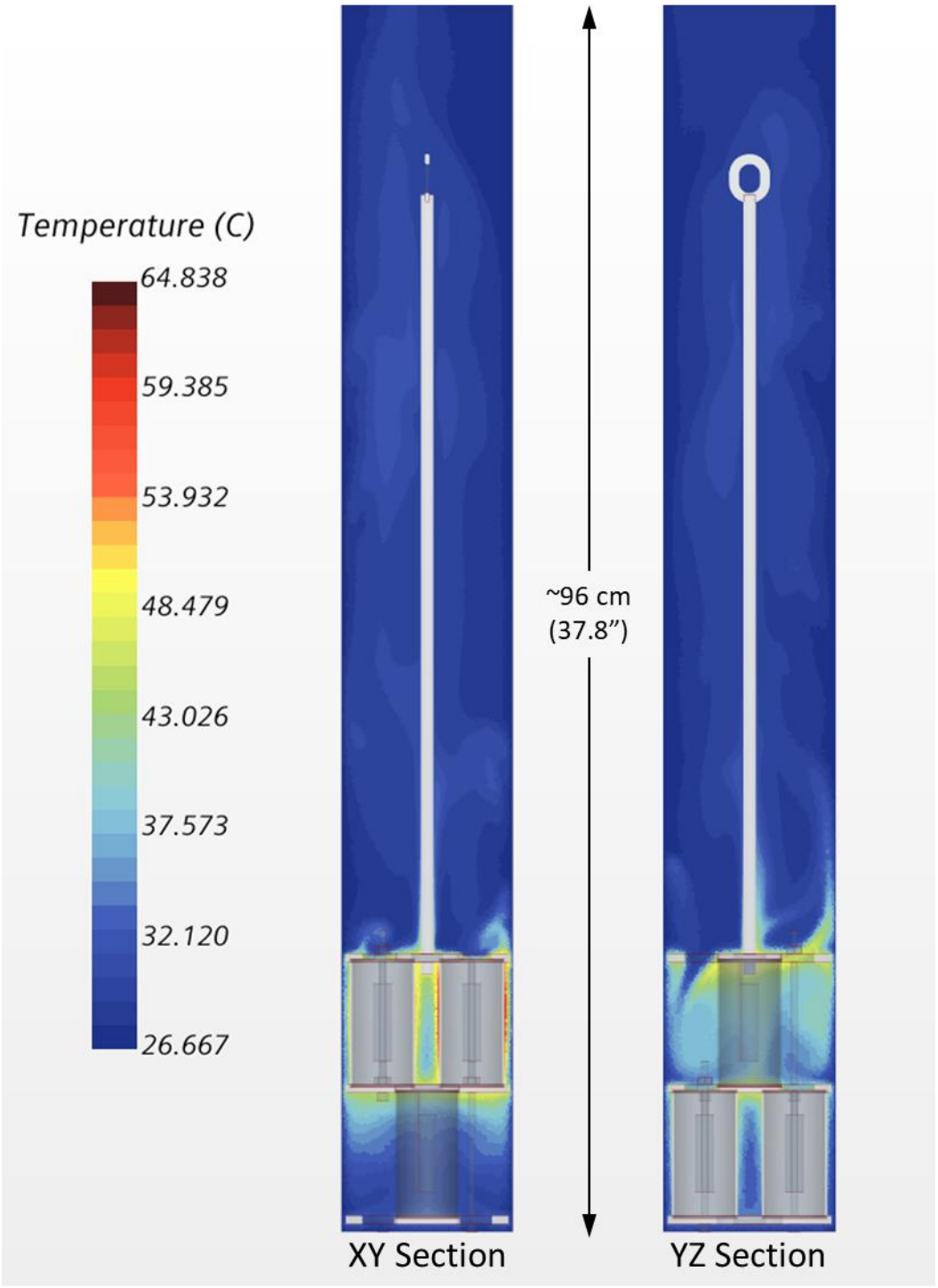

Figure 28. Target Temperature Case – XY and YZ cross sections of air temperature around the experiment assembly.

6.7.2 High Temperature Case

When the temperature inside the insulation of the four inner baskets is increased to 800°C, the temperature of the bottom lead cap increases to about 27.5°C as shown in Figure 29. This is a negligible increase of only ~0.6°C from the target temperature case. Similarly, the maximum temperature of the gamma tube's interior wall increases to only ~29.5°C (Figure 30) or ~1.7°C higher than the target temperature case.

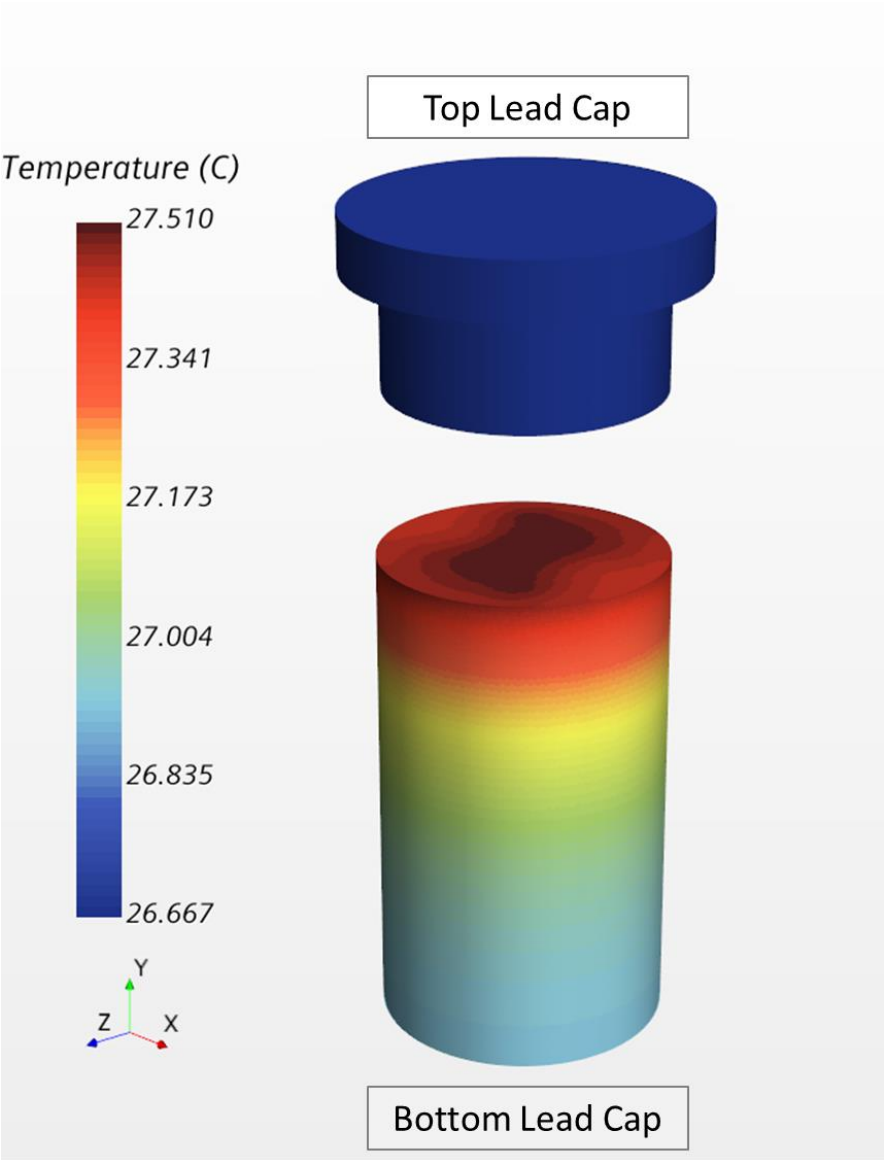

Figure 29. High Temperature Case – temperature of the top and bottom lead caps.

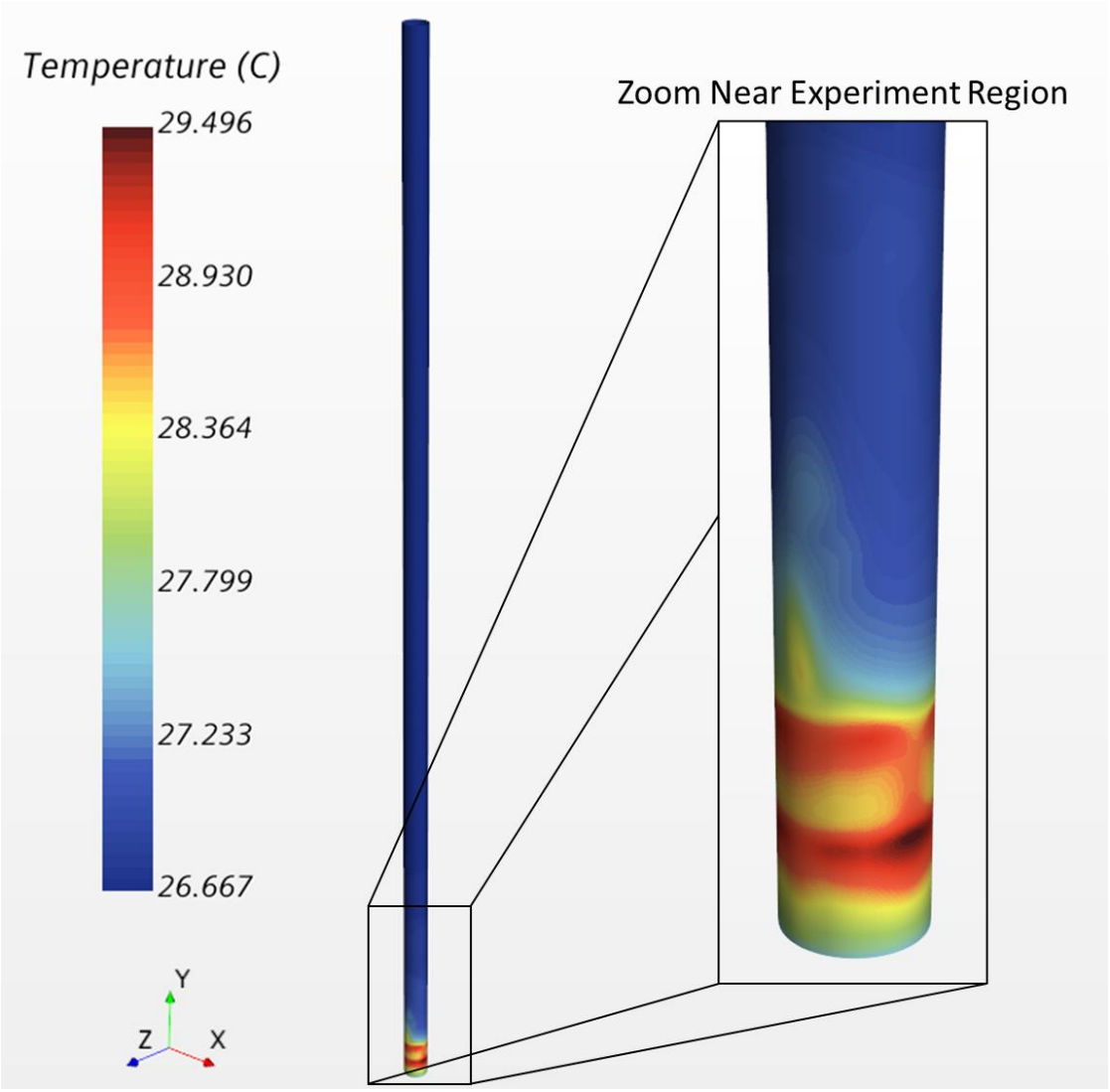

Figure 30. High Temperature Case – temperature of the gamma tube's internal walls with zoomed view near the experiment.

Cross sections of air temperature through the top and bottom sets of inner baskets are shown in Figure 31. As expected, the air temperature around the inner baskets is higher in the high temperature case with temperatures approaching 110°C near the top surfaces of the insulation. Overall, the air temperature is much higher than the target temperature case with the bulk of the air volume around the lower set of inner baskets varying from about 40 to 80°C.

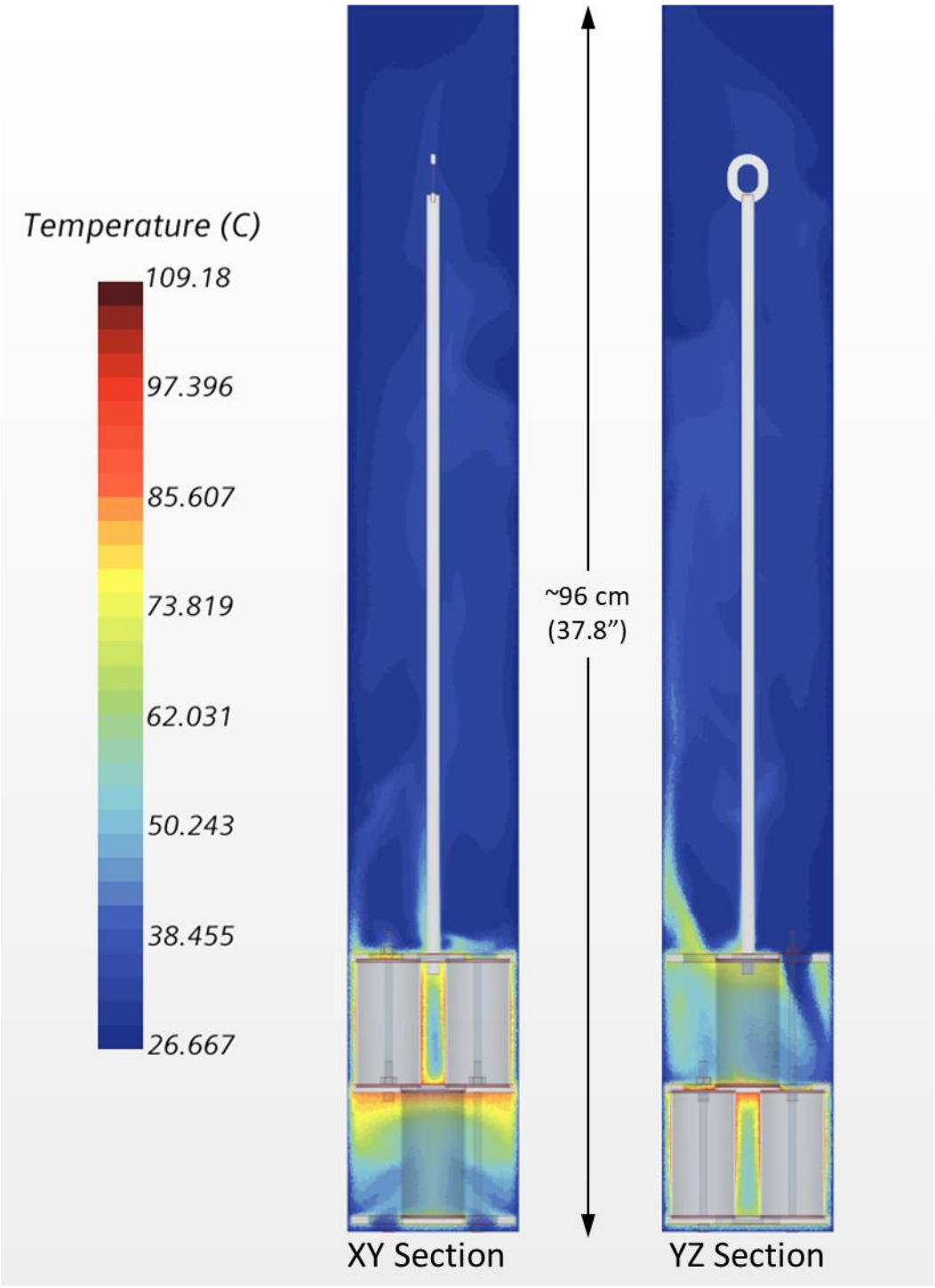

Figure 31. High Temperature Case – XY and YZ cross sections of air temperature around the experiment assembly.

6.8 Conclusion

A conjugate heat transfer model of the experiment was developed in Star-CCM+. Two cases were explored: the target temperature case which, as the name suggests, utilized the experiment's target

temperatures and a second, high temperature case where the temperatures were increased to the upper limit of the available material properties. Table 4 provides a summary of the results of these two cases. Overall, the temperatures of the gamma tube components are only negligibly affected by the expected range of experiment temperatures.

Table 4. Summary of analysis results.

	Maximum Temperature (°C)		
Case	**Lead Caps**	**Gamma Tube Walls**	**Air Temperature**
Target Temperature	26.9	27.8	64.8
High Temperature	27.5	29.5	109.2

References used in this ECAR

SHawkes, B. D. (2015). *ECAR-2741 Drop Analysis of the GE-2000 Cask Insert in the ATR Canal Area.* Idaho National Laboratory.

Incropera, F. P., & DeWitt, D. P. (2002). *Fundamentals of Heat and Mass Transfer, 5th Edition.* New York: John Wiley & Sons.

Kennedy, J. C. (2018). *ECAR-4345 Hot cell feedthrough analysis.*

Morgan Advanced Materials. (2019, 12 09). *Data Sheet - WDS Shape.* Retrieved 01 06, 2021, from https://www.morganthermalceramics.com/media/7561/wds-shape_eng.pdf

(2016). *PLN-3597, Enterprise Engineering/Scientific Software, Rev 6.* Idaho National Laboratory.

Star-CCM+ 14.06.013-R8. (2019). Melville, NY: CD-Adapco.

Xing, C. (2020). *ECAR-4957 Thermal Analysis of the BSU-8242 and N-SERT Capsule Shipment in the BRR Cask Using a CFD Approach.*

7. Appendix B: GASR Analysis of the Salt Capsules.

HFEF Tracking NO.: 2-5423 **Specimen ID: TPRC-01 First Analysis**

Specimen Type:	ATR Salt Radiolysis container
ID Number:	TPRC-01
MTG ID Number:	TPRC-01
Diameter:	0.375
Wall Thickness:	0.02
Length:	3.17
DWG Number:	1004226
Estimated Sample Gas Press:	12.2
Aux. Volume:	None
Transducer:	PI-023 (0-15)
Focus Position (Turns):	9.5
Laser Configuration:	
Drilling:	
Burst 1, .02 inch thick: Pulse Width 750 micro-sec, 1125 mJ, 1500W, 6 pulses;	
Welding:	
Burst 3, .02 inch thick: Pulse Width 600 micro-sec, 900 mJ, 1500W, 6 pulses;	
focus lens at 9.7/.797 inch	

PRE-USE INSPECTIONS

Iteration		Date	Time	Initial PE-023	Final PE-023	Vsh	Vm	Initial PE-024	Final PE-024	Vsh	Vm	TE-044	TE-042	TE-043
	1	1/26/2022	10:09:56 AM	4.9316	2.1115	59.1009	80.2163	4.9463	2.127	59.5494	79.6121	23	23.9	21.4
	2	1/26/2022	10:12:46 AM	6.9272	2.9738	59.3754	79.8454	6.9458	2.9881	59.5941	79.5524	23	23.8	21.4
	3	1/26/2022	10:16:07 AM	9.93	4.2713	59.5822	79.5683	9.9452	4.2842	59.7361	79.3633	23	23.8	21.4
	4	1/26/2022	10:19:44 AM	11.9295	5.1866	59.6876	79.4278	11.9482	5.1501	59.798	79.2811	23.1	23.7	21.4
	5	1/26/2022	10:23:49 AM	14.9265	6.4341	59.8027	79.275	14.9466	6.448	59.8885	79.1613	23.2	23.7	21.4

POST PUNCTURE AND CAPSULE GAS EXPANSION

Sample	Date	Time	Pex	PE-021	PE-024	PE-026	TE-044	TE-042	TE-043
Puncture	1/26/2022	10:48:39 AM	0.4571	0.4571	---------	---------	23.52	23.79	21.52
Manifold	1/26/2022	10:49:56 AM	-------	0.1743	0.1966	-0.139	23.54	23.81	21.53
Sample Tubing	1/26/2022	10:50:06 AM	-------	0.1752	0.1809	-0.136	23.54	23.81	21.53
Sample Bottle Pressure	1/26/2022	10:50:29 AM	-------	0.1767	0.0589	-0.0758	23.54	23.82	21.53

BACKFILL/EXPANSIONS

Iteration		Date	Time	Initial PE-023	Final PE-023	Vpin PE-023	Ppin PE-023	Initial PE-024	Final PE-024	Vpin PE-024	Ppin PE-024	TE-44	TE-42	TE-43
	1	1/26/2022	11:07:11 AM	6.9258	3.0537	2.189	12.9977	6.9438	3.0714	2.5448	11.244	23.8	24	21.6
	2	1/26/2022	11:10:05 AM	6.9246	3.0532	2.192	12.9802	6.9434	3.07	2.4998	11.4383	23.9	24	21.6
	3	1/26/2022	11:12:57 AM	6.9293	3.0546	2.1669	13.1253	6.9486	3.074	2.5638	11.1641	23.7	24	21.6
	4	1/26/2022	11:15:45 AM	6.9331	3.056	2.1547	13.1973	6.9503	3.0742	2.5424	11.2542	23.4	24	21.6
	5	1/26/2022	11:18:37 AM	6.9238	3.0502	2.0935	13.5697	6.9447	3.0656	2.3206	12.2863	23.1	23.9	21.6
	6	1/26/2022	11:22:04 AM	9.9266	4.3849	2.3943	11.9221	9.9455	4.4006	2.5843	11.0792	22.7	23.7	21.7
	7	1/26/2022	11:25:23 AM	9.9271	4.3843	2.3738	12.0214	9.9423	4.4001	2.6073	10.9856	22.5	23.6	21.7
	8	1/26/2022	11:28:41 AM	9.928	4.3841	2.3605	12.0861	9.9465	4.4011	2.5835	11.0826	22.5	23.5	21.6
	9	1/26/2022	11:32:00 AM	9.9223	4.3828	2.391	11.9381	9.9401	4.3947	2.495	11.4596	22.5	23.4	21.6
	10	1/26/2022	11:35:27 AM	9.9279	4.385	2.3843	11.9702	9.9449	4.4003	2.5831	11.0841	22.5	23.4	21.6
	11	1/26/2022	11:39:10 AM	11.9324	5.2755	2.4934	11.4665	11.9475	5.2898	2.6549	10.7966	22.6	23.3	21.6
	12	1/26/2022	11:42:52 AM	11.932	5.2758	2.5039	11.4205	11.9489	5.2884	2.6123	10.9655	22.6	23.3	21.6
	13	1/26/2022	11:46:35 AM	11.9292	5.2742	2.496	11.455	11.9475	5.2871	2.5969	11.0278	22.7	23.3	21.6
	14	1/26/2022	11:50:16 AM	11.9312	5.2762	2.5186	11.3565	11.9453	5.2887	2.6533	10.8032	22.8	23.3	21.6
	15	1/26/2022	11:53:59 AM	11.9286	5.2756	2.5314	11.3013	11.9444	5.2893	2.6733	10.7258	22.8	23.3	21.6
	16	1/26/2022	11:58:11 AM	14.9316	6.6086	2.6131	10.9623	14.9485	6.623	2.7309	10.5092	22.8	23.4	21.6
	17	1/26/2022	12:02:25 PM	14.9326	6.6098	2.6268	10.9074	14.9458	6.6229	2.7505	10.4372	22.9	23.4	21.6
	18	1/26/2022	12:06:31 PM	14.9308	6.6099	2.6426	10.845	14.949	6.6234	2.7348	10.4948	23	23.4	21.5
	19	1/26/2022	12:10:46 PM	14.936	6.6094	2.5946	11.0371	14.9497	6.6217	2.7015	10.6184	23	23.5	21.5
	20	1/26/2022	12:14:58 PM	14.9316	6.6105	2.6464	10.8301	14.9456	6.6217	2.7323	10.5038	23.1	23.5	21.5

SYSTEM CALCULATED AVERAGES

Average PE-023 Vsh	Average PE-023 Vm	Average PE-024 Vsh	Average PE-024 Vm	Average PE-023 Vpin	Average PE-024 Vpin	Average PE-023 Ppin	Average PE-024 Ppin
59.5098	79.6666	59.7132	79.394	2.4183	2.6083	11.8695	10.998

Calculated Capsule Volume	2.4183	cc
Calculated Capsule Internal Pressure	11.8695	psia

PE-023 is a 0-15 psia gauge with a +/- 0.05% Full Scale Accuracy
PE-024 is a 0-50 psia gauge with a +/- 0.05% Full Scale Accuracy
The results calculated from PE-023 are expected to be more accurate than those from PE-024

HFEF Tracking NO.: 2-5423 **Specimen ID: TPRC-01 Second Analysis**

Specimen Type:	**ATR Salt Radiolysis container**
ID Number:	**TPRC-01**
MTG ID Number:	**TPRC-01**
Diameter:	0.375
Wall Thickness:	0.02
Length:	3.17
DWG Number:	1004226
Estimated Sample Gas Press:	14.958
Aux. Volume:	None
Transducer:	PI-023 (0-15)
Focus Position (Turns):	9.5
Laser Configuration:	
Drilling:	
Burst 1, .02 inch thick: Pulse Width 750 micro-sec, 1125 mJ, 1500W, 6 pulses.	
Welding:	
Burst 3, .02 inch thick: Pulse Width 600 micro-sec, 900 mJ, 1500W, 6 pulses.	
focus lens at 9.7/.797 inch	

PRE-USE INSPECTIONS

Iteration	Date	Time	Initial PE-023	Final PE-023	Vsh	Vm	Initial PE-024	Final PE-024	Vsh	Vm	TE-044	TE-042	TE-043
1	1/27/2022	7:45:55 AM	4.9204	2.1037	58.9553	80.4144	4.942	2.1222	59.4046	79.8061	23.7	24	20.8
2	1/27/2022	7:48:50 AM	6.9249	2.9706	59.2971	79.9509	6.9454	2.9927	59.7645	79.3256	23.4	23.9	20.8
3	1/27/2022	7:52:12 AM	9.9207	4.2677	59.591	79.5566	9.9441	4.288	59.842	79.2228	22.9	23.7	20.8
4	1/27/2022	7:55:48 AM	11.9268	5.1338	59.6535	79.4733	11.9503	5.1555	59.891	79.1581	22.5	23.6	20.8
5	1/27/2022	7:59:58 AM	14.9223	6.4302	59.768	79.321	14.9471	6.4522	59.9535	79.0756	22.5	23.5	20.8

POST PUNCTURE AND CAPSULE GAS EXPANSION

Sample	Date	Time	Pex	PE-021	PE-024	PE-026	TE-044	TE-042	TE-043
Puncture	1/27/2022	9:13:01 AM	0.4408	0.4408	---------	--------	23.88	23.97	21.6
Manifold	1/27/2022	9:14:28 AM	---------	0.165	0.1915	-0.1395	23.91	24.04	21.62
Sample Tubing	1/27/2022	9:14:38 AM	---------	0.1651	0.087	-0.1293	23.91	24.05	21.62
Sample Bottle Pressure	1/27/2022	9:14:57 AM	---------	0.1656	0.043	-0.0698	23.92	24.07	21.62

BACKFILL/EXPANSIONS

Iteration	Date	Time	Initial PE-023	Final PE-023	Vpin PE-023	Ppin PE-023	Initial PE-024	Final PE-024	Vpin PE-024	Ppin PE-024	TE-44	TE-42	TE-43
1	1/27/2022	9:20:41 AM	6.9175	3.0454	2.0206	13.5431	6.9417	3.0689	2.4886	11.0791	24	24.2	21.7
2	1/27/2022	9:23:36 AM	6.921	3.0463	1.9973	13.6958	6.9444	3.0672	2.3825	11.5529	24.1	24.2	21.7
3	1/27/2022	9:26:34 AM	6.9272	3.0497	2.0228	13.5285	6.9506	3.0703	2.3975	11.4834	24.1	24.2	21.7
4	1/27/2022	9:29:31 AM	6.9194	3.0454	1.9899	13.745	6.9443	3.068	2.4139	11.4082	24.2	24.3	21.7
5	1/27/2022	9:32:31 AM	6.9222	3.046	1.9687	13.8881	6.9483	3.0694	2.3975	11.4833	24.2	24.3	21.7
6	1/27/2022	9:35:56 AM	9.9269	4.3829	2.3404	11.7527	9.9495	4.4021	2.576	10.7181	24.3	24.4	21.7
7	1/27/2022	9:39:20 AM	9.9221	4.3804	2.3317	11.7949	9.9445	4.4001	2.5811	10.6976	24.4	24.5	21.7
8	1/27/2022	9:42:45 AM	9.9207	4.3804	2.3489	11.7118	9.9434	4.4041	2.6954	10.2628	24.5	24.5	21.7
9	1/27/2022	9:46:09 AM	9.928	4.3833	2.3398	11.7558	9.9503	4.3994	2.4989	11.0351	24.6	24.6	21.7
10	1/27/2022	9:49:33 AM	9.9231	4.3812	2.3419	11.7452	9.9476	4.4005	2.5562	10.7975	24.3	24.6	21.7
11	1/27/2022	9:53:20 AM	11.9254	5.2695	2.4305	11.3336	11.95	5.2862	2.5561	10.7982	23.7	24.5	21.7
12	1/27/2022	9:57:00 AM	11.9294	5.2709	2.4232	11.3662	11.9483	5.2883	2.6149	10.5652	23.2	24.3	21.6
13	1/27/2022	10:00:41 AM	11.9258	5.2684	2.4046	11.4507	11.9499	5.2855	2.5412	10.8588	22.8	24	21.6
14	1/27/2022	10:04:20 AM	11.924	5.2683	2.4195	11.383	11.9461	5.2833	2.5295	10.9071	22.5	23.8	21.6
15	1/27/2022	10:08:01 AM	11.9308	5.2712	2.416	11.3985	11.9521	5.2905	2.6264	10.5209	22.3	23.6	21.6
16	1/27/2022	10:12:12 AM	14.9319	6.602	2.4996	11.0324	14.9548	6.62	2.6341	10.4915	22.3	23.5	21.5
17	1/27/2022	10:16:25 AM	14.9279	6.6021	2.5309	10.901	14.9499	6.6203	2.6748	10.3384	22.3	23.4	21.5
18	1/27/2022	10:20:38 AM	14.9321	6.6033	2.5201	10.946	14.9528	6.6202	2.651	10.4274	22.4	23.3	21.5
19	1/27/2022	10:24:53 AM	14.9313	6.6044	2.545	10.8432	14.9507	6.6197	2.6597	10.3947	22.4	23.3	21.5
20	1/27/2022	10:29:05 AM	14.9365	6.6078	2.5638	10.7668	14.9548	6.6202	2.6369	10.4807	22.5	23.3	21.4

SYSTEM CALCULATED AVERAGES

Average PE-023 Vsh	Average PE-023 Vm	Average PE-024 Vsh	Average PE-024 Vm	Average PE-023 Vpin	Average PE-024 Vpin	Average PE-023 Ppin	Average PE-024 Ppin
59.453	79.7432	59.7711	79.3176	2.3228	2.5556	11.9291	10.815

Calculated Capsule Volume	2.3228	cc
Calculated Capsule Internal Pressure	11.9291	psia

PE-023 is a 0-15 psia gauge with a +/- 0.05% Full Scale Accuracy
PE-024 is a 0-50 psia guage with a +/- 0.05% Full Scale Accuracy
The results calculated from PE-023 are expected to be more accurate than those from PE-024
The initial capsule fill pressure after welding was 14.958 psia.
The time between charging to 14.958 psia and subsequent drilling and volume analysis was approximately 18 hrs.

HFEF Tracking NO.: 2-5423

Specimen ID: TPRC-02 First Analysis

Specimen Type:	**ATR Salt Radiolysis container**
ID Number:	**TPRC-02**
MTG ID Number:	**TPRC-02**
Diameter:	0.375
Wall Thickness:	0.02
Length:	3.17
DWG Number:	1004226
Estimated Sample Gas Press:	12.2
Aux. Volume:	None
Transducer:	PI-023 (0-15)
Focus Position (Turns):	9.5
Laser Configuration:	
Drilling:	
Burst 1, .02 inch thick: Pulse Width 750 micro-sec, 1125 mJ, 1500W, 6 pulses.	
Welding:	
Burst 3, .02 inch thick: Pulse Width 600 micro-sec, 900 mJ, 1500W, 6 pulses.	
focus lens at 9.7/.797 inch	

Iteration	Date	Time	Initial PE-023	Final PE-023	Vsh	Vm	Initial PE-024	Final PE-024	Vsh	Vm	TE-044	TE-042	TE-043
1	1/27/2022	11:23:02 AM	4.9291	2.1096	59.0622	80.2689	4.9462	2.1277	59.5868	79.5622	23.6	23.9	21.3
2	1/27/2022	11:25:55 AM	6.9306	2.9758	59.3929	79.8218	6.9485	2.9863	59.4911	79.6902	23.7	24	21.3
3	1/27/2022	11:29:19 AM	9.9346	4.2739	59.5973	79.5482	9.9519	4.2899	59.8053	79.2714	23.7	24	21.3
4	1/27/2022	11:33:04 AM	11.9282	5.1387	59.7427	79.3546	11.9467	5.1546	59.9038	79.1412	23.8	24.1	21.3
5	1/27/2022	11:37:16 AM	14.928	6.4364	59.8302	79.2385	14.9487	6.4522	59.9418	79.091	23.9	24.1	21.3

Sample	Date	Time	Pex	PE-021	PE-024	PE-026	TE-044	TE-042	TE-043
Puncture	1/27/2022	1:24:13 PM	0.4409	0.4409	---------	---------	23.55	23.88	22.22
Manifold	1/27/2022	1:25:15 PM	---------	0.1662	0.187	-0.1396	23.56	23.92	22.22
Sample Tubing	1/27/2022	1:25:24 PM	---------	0.1664	0.1726	-0.136	23.56	23.92	22.23
Sample Bottle Pressure	1/27/2022	1:25:47 PM	---------	0.1657	0.0511	-0.0747	23.57	23.93	22.23

Iteration	Date	Time	Initial PE-023	Final PE-023	Vpin PE-023	Ppin PE-023	Initial PE-024	Final PE-024	Vpin PE-024	Ppin PE-024	TE-44	TE-42	TE-43
1	1/27/2022	1:32:28 PM	6.9183	3.0483	2.1116	12.9825	6.9364	3.0686	2.5615	10.7795	23.6	24	22.3
2	1/27/2022	1:35:24 PM	6.9257	3.0507	2.0834	13.152	6.9464	3.0687	2.4044	11.4552	23.7	24	22.3
3	1/27/2022	1:38:13 PM	6.9277	3.0514	2.077	13.1913	6.9491	3.0715	2.4652	11.1834	23.7	24.1	22.3
4	1/27/2022	1:41:10 PM	6.9238	3.0495	2.0668	13.2542	6.9441	3.0678	2.4098	11.4305	23.8	24.1	22.3
5	1/27/2022	1:44:04 PM	6.9222	3.048	2.039	13.4291	6.945	3.0668	2.3585	11.6694	23.8	24.1	22.3
6	1/27/2022	1:47:27 PM	9.9292	4.3848	2.3638	11.6442	9.9465	4.4002	2.5609	10.782	23.8	24.2	22.3
7	1/27/2022	1:50:49 PM	9.9258	4.3832	2.3611	11.6571	9.9455	4.4026	2.6343	10.4937	23.9	24.2	22.3
8	1/27/2022	1:54:03 PM	9.9302	4.3856	2.3718	11.6064	9.9508	4.4022	2.5643	10.7684	23.9	24.2	22.3
9	1/27/2022	1:57:28 PM	9.9268	4.3831	2.3475	11.7218	9.9431	4.3985	2.5573	10.7967	24	24.3	22.2
10	1/27/2022	2:00:44 PM	9.9193	4.3789	2.3238	11.8373	9.94	4.3981	2.5812	10.7006	24	24.3	22.2
11	1/27/2022	2:04:21 PM	11.9298	5.2737	2.4793	11.1225	11.9495	5.2915	2.6729	10.3485	24.1	24.3	22.2
12	1/27/2022	2:07:59 PM	11.9268	5.2719	2.4688	11.1678	11.9443	5.2882	2.6507	10.4316	24.1	24.4	22.1
13	1/27/2022	2:11:42 PM	11.9286	5.2726	2.4676	11.1732	11.9507	5.2918	2.6677	10.3678	24.1	24.4	22.1
14	1/27/2022	2:15:20 PM	11.9295	5.2721	2.4479	11.2592	11.9493	5.2918	2.6808	10.3196	24.2	24.5	22.1
15	1/27/2022	2:18:59 PM	11.9277	5.273	2.4848	11.0988	11.95	5.2899	2.6342	10.4942	24.2	24.5	22
16	1/27/2022	2:23:09 PM	14.9278	6.6053	2.5857	10.6826	14.9494	6.6232	2.7291	10.1447	24.3	24.5	22
17	1/27/2022	2:27:25 PM	14.9267	6.6062	2.6097	10.5885	14.9497	6.6278	2.8037	9.8866	24.4	24.6	21.9
18	1/27/2022	2:31:33 PM	14.9252	6.6055	2.6087	10.5925	14.9472	6.6265	2.802	9.8921	24.5	24.7	21.9
19	1/27/2022	2:35:44 PM	14.9283	6.6042	2.5645	10.7677	14.9505	6.6228	2.7126	10.2035	24.5	24.7	21.9
20	1/27/2022	2:39:51 PM	14.9232	6.6019	2.5624	10.7758	14.9472	6.6215	2.7158	10.1921	24.6	24.8	21.8

Average PE-023 Vsh	Average PE-023 Vm	Average PE-024 Vsh	Average PE-024 Vm	Average PE-023 Vpin	Average PE-024 Vpin	Average PE-023 Ppin	Average PE-024 Ppin
59.5251	79.6464	59.7458	79.3512	2.3713	2.6083	11.6852	10.617

Calculated Capsule Volume	2.3713	cc
Calculated Capsule Internal Pressure	11.6852	psia

PE-023 is a 0-15 psia gauge with a +/- 0.05% Full Scale Accuracy

PE-024 is a 0-50 psia guage with a +/- 0.05% Full Scale Accuracy

The results calculated from PE-023 are expected to be more accurate than those from PE-024

TPRC-02 was not able to be welded. No second analysis was performed.

HFEF Tracking NO.: 2-5423

Specimen ID: TPRC-03 First Analysis

Specimen Type:	**ATR Salt Radiolysis container**
ID Number:	**TPRC-03**
MTG ID Number:	**TPRC-03**
Diameter:	0.375
Wall Thickness:	0.02
Length:	3.17
DWG Number:	1004226
Estimated Sample Gas Press:	12.2
Aux. Volume:	None
Transducer:	PI-023 (0-15)
Focus Position (Turns):	9.5
Laser Configuration:	
Drilling:	
Burst 1, .02 inch thick: Pulse Width 750 micro-sec, 1125 mJ, 1500W, 6 pulses.	
Welding:	
Burst 3, .02 inch thick: Pulse Width 600 micro-sec, 900 mJ, 1500W, 6 pulses.	
focus lens at 9.7/.797 inch	

PRE-USE INSPECTIONS

Iteration		Date	Time	Initial PE-023	Final PE-023	Vsh	Vm	Initial PE-024	Final PE-024	Vsh	Vm	TE-044	TE-042	TE-043
	1	2/1/2022	9:24:28 AM	4.9186	2.1075	59.1793	80.1101	4.9375	2.1253	59.6526	79.4744	22.2	22.6	20.8
	2	2/1/2022	9:27:23 AM	6.9335	2.98	59.4966	79.6828	6.9527	2.9972	59.8118	79.2629	22.2	22.6	20.8
	3	2/1/2022	9:30:51 AM	9.9308	4.2762	59.692	79.4219	9.9536	4.2881	59.7439	79.3529	22.1	22.6	20.9
	4	2/1/2022	9:34:29 AM	11.9334	5.1432	59.7877	79.2948	11.951	5.1598	59.9718	79.0514	22.1	22.6	20.9
	5	2/1/2022	9:38:36 AM	14.9323	6.4405	59.8661	79.191	14.9516	6.4556	59.9781	79.0431	22.2	22.6	20.9

POST PUNCTURE AND CAPSULE GAS EXPANSION

Sample	Date	Time	Pex	PE-021	PE-024	PE-026	TE-044	TE-042	TE-043
Puncture	2/1/2022	10:13:58 AM	0.4404	0.4404	---------	---------	21.99	22.62	21.14
Manifold	2/1/2022	10:14:41 AM	---------	0.1727	0.1912	-0.139	22	22.63	21.15
Sample Tubing	2/1/2022	10:14:50 AM	---------	0.1727	0.1795	-0.1375	22	22.63	21.15
Sample Bottle Pressure	2/1/2022	10:15:13 AM	---------	0.1734	0.0538	-0.0746	22.01	22.63	21.16

BACKFILL/EXPANSIONS

Iteration		Date	Time	Initial PE-023	Final PE-023	Vpin PE-023	Ppin PE-023	Initial PE-024	Final PE-024	Vpin PE-024	Ppin PE-024	TE-44	TE-42	TE-43
	1	2/1/2022	10:21:54 AM	6.9195	3.0549	2.3362	11.7623	6.9371	3.0742	2.7583	10.0298	22.1	22.7	21.2
	2	2/1/2022	10:24:48 AM	6.9291	3.0584	2.3071	11.9052	6.948	3.073	2.5372	10.8656	22.2	22.7	21.3
	3	2/1/2022	10:27:42 AM	6.9287	3.058	2.3007	11.9371	6.9448	3.0768	2.7249	10.1473	22.3	22.7	21.3
	4	2/1/2022	10:30:35 AM	6.9278	3.0575	2.2967	11.9571	6.9433	3.0716	2.5612	10.7677	22.4	22.7	21.3
	5	2/1/2022	10:33:29 AM	6.9268	3.0566	2.2809	12.0367	6.9454	3.0706	2.4901	11.0629	22.4	22.8	21.3
	6	2/1/2022	10:36:53 AM	9.9263	4.3894	2.5143	10.9606	9.945	4.4039	2.6746	10.33	22.5	22.8	21.3
	7	2/1/2022	10:40:23 AM	9.9333	4.3934	2.5377	10.8634	9.949	4.4068	2.7021	10.2292	22.5	22.9	21.3
	8	2/1/2022	10:43:44 AM	9.9273	4.3889	2.4897	11.0645	9.9416	4.4037	2.7062	10.2146	22.5	22.9	21.3
	9	2/1/2022	10:47:09 AM	9.9258	4.3897	2.5271	10.9071	9.9467	4.4063	2.7157	10.1803	22.6	22.9	21.3
	10	2/1/2022	10:50:33 AM	9.9245	4.3901	2.5524	10.8032	9.9412	4.407	2.7965	9.8987	22.6	23	21.3
	11	2/1/2022	10:54:12 AM	11.9298	5.2789	2.5895	10.655	11.9464	5.2911	2.6925	10.2643	22.6	23	21.3
	12	2/1/2022	10:57:52 AM	11.9298	5.2806	2.625	10.5168	11.9501	5.2935	2.7087	10.2054	22.7	23	21.3
	13	2/1/2022	11:01:30 AM	11.9277	5.28	2.6335	10.4844	11.9441	5.2899	2.689	10.2772	22.8	23.1	21.3
	14	2/1/2022	11:05:08 AM	11.9275	5.2795	2.6241	10.5204	11.9429	5.2924	2.7529	10.0488	22.8	23.1	21.3
	15	2/1/2022	11:08:54 AM	11.9285	5.2774	2.571	10.7287	11.9454	5.2897	2.6719	10.3401	22.9	23.2	21.3
	16	2/1/2022	11:13:14 AM	14.9342	6.6148	2.6999	10.2372	14.9513	6.6286	2.8052	9.8696	23	23.2	21.3
	17	2/1/2022	11:17:26 AM	14.9273	6.6127	2.7155	10.1809	14.9447	6.6264	2.8177	9.8278	23.1	23.3	21.3
	18	2/1/2022	11:21:31 AM	14.936	6.6165	2.715	10.1829	14.9531	6.6321	2.8521	9.7144	23.2	23.3	21.3
	19	2/1/2022	11:25:46 AM	14.9408	6.6177	2.7006	10.2349	14.9547	6.6305	2.8119	9.8471	23.2	23.4	21.3
	20	2/1/2022	11:29:59 AM	14.9356	6.6161	2.7111	10.1967	14.9497	6.6277	2.8031	9.8766	23.3	23.6	21.3

SYSTEM CALCULATED AVERAGES

Average PE-023 Vsh	Average PE-023 Vm	Average PE-024 Vsh	Average PE-024 Vm	Average PE-023 Vpin	Average PE-024 Vpin	Average PE-023 Ppin	Average PE-024 Ppin
59.6043	79.5401	59.8316	79.2369	2.5364	2.7136	10.9068	10.1999

Calculated Capsule Volume	2.5364	cc
Calculated Capsule Internal Pressure	10.9068	psia

PE-023 is a 0-15 psia gauge with a +/- 0.05% Full Scale Accuracy
PE-024 is a 0-50 psia guage with a +/- 0.05% Full Scale Accuracy
The results calculated from PE-023 are expected to be more accurate than those from PE-024

HFEF Tracking NO.: 2-5423

Specimen ID: TPRC-03 Second Analysis

Specimen Type:	**ATR Salt Radiolysis container**
ID Number:	**TPRC-03**
MTG ID Number:	**TPRC-03**
Diameter:	0.375
Wall Thickness:	0.02
Length:	3.17
DWG Number:	1004226
Estimated Sample Gas Press:	14.955
Aux. Volume:	None
Transducer:	PI-023 (0-15)
Focus Position (Turns):	9.5
Laser Configuration:	
Drilling:	
Burst 1, .02 inch thick: Pulse Width 750 micro-sec, 1125 mJ, 1500W, 6 pulses.	
Welding:	
Burst 3, .02 inch thick: Pulse Width 600 micro-sec, 900 mJ, 1500W, 6 pulses.	
focus lens at 9.7/.797 inch	

PRE-USE INSPECTIONS

Iteration		Date	Time	Initial PE-023	Final PE-023	Vsh	Vm	Initial PE-024	Final PE-024	Vsh	Vm	TE-044	TE-042	TE-043
	1	2/1/2022	1:57:04 PM	4.926	2.1039	58.8483	80.5606	4.9505	2.127	59.4643	79.726	24.7	26.4	21
	2	2/1/2022	1:59:59 PM	6.9179	2.9675	59.2938	79.9553	6.9447	2.9877	59.5992	79.5456	24.7	26.4	21
	3	2/1/2022	2:03:23 PM	9.9279	4.2714	59.6059	79.5366	9.9526	4.2936	59.8889	79.1608	24.7	26.4	21
	4	2/1/2022	2:06:57 PM	11.9182	5.1332	59.7187	79.3865	11.9449	5.1568	59.9658	79.0594	24.7	26.4	21
	5	2/1/2022	2:11:09 PM	14.9208	6.4342	59.8445	79.2196	14.9488	6.4551	59.9894	79.0282	24.8	26.5	21

POST PUNCTURE AND CAPSULE GAS EXPANSION

Sample	Date	Time	Pex	PE-021	PE-024	PE-026	TE-044	TE-042	TE-043
Puncture	2/1/2022	2:24:04 PM	0.5726	0.5726	---------	---------	24.81	26.53	21.06
Manifold	2/1/2022	2:24:47 PM	---------	0.219	0.2434	-0.1402	24.82	26.56	21.06
Sample Tubing	2/1/2022	2:24:56 PM	---------	0.2194	0.1059	-0.1274	24.82	26.57	21.06
Sample Bottle Pressure	2/1/2022	2:25:16 PM	---------	0.2203	0.0524	-0.0508	24.82	26.58	21.07

BACKFILL/EXPANSIONS

Iteration		Date	Time	Initial PE-023	Final PE-023	Vpin PE-023	Ppin PE-023	Initial PE-024	Final PE-024	Vpin PE-024	Ppin PE-024	TE-44	TE-42	TE-43
	1	2/1/2022	2:31:38 PM	6.9193	3.0455	1.9962	17.8007	6.9474	3.0701	2.4411	14.6613	24.8	26.6	21.1
	2	2/1/2022	2:34:38 PM	6.9194	3.0456	1.9965	17.7982	6.9433	3.0678	2.4214	14.776	24.9	26.6	21.1
	3	2/1/2022	2:37:30 PM	6.9214	3.0461	1.9825	17.9197	6.9466	3.0678	2.3693	15.088	24.9	26.7	21.1
	4	2/1/2022	2:40:31 PM	6.9257	3.0482	1.9915	17.8418	6.9501	3.0701	2.3981	14.9138	24.9	26.7	21.2
	5	2/1/2022	2:43:24 PM	6.9235	3.0465	1.9666	18.0601	6.9463	3.0675	2.3631	15.1259	24.9	26.7	21.2
	6	2/1/2022	2:46:54 PM	9.9254	4.3832	2.3662	15.1069	9.9483	4.4035	2.6256	13.671	24.9	26.7	21.2
	7	2/1/2022	2:50:24 PM	9.9194	4.3805	2.3652	15.1134	9.9441	4.4023	2.6429	13.5856	24.9	26.8	21.2
	8	2/1/2022	2:53:40 PM	9.9235	4.382	2.3572	15.1628	9.9474	4.4044	2.658	13.5115	24.9	26.8	21.2
	9	2/1/2022	2:57:04 PM	9.9265	4.3836	2.3642	15.1196	9.954	4.4032	2.5542	14.0374	25	26.8	21.2
	10	2/1/2022	3:00:18 PM	9.922	4.3815	2.3604	15.1429	9.9447	4.4063	2.7382	13.1325	25	26.9	21.2
	11	2/1/2022	3:04:01 PM	11.924	5.272	2.4978	14.3416	11.9535	5.2956	2.7222	13.2065	25	26.9	21.2
	12	2/1/2022	3:07:44 PM	11.9154	5.2679	2.4909	14.3795	11.9447	5.2913	2.7138	13.2452	25	27	21.2
	13	2/1/2022	3:11:24 PM	11.9141	5.2681	2.5074	14.2887	11.9417	5.2886	2.6835	13.3886	25	27	21.2
	14	2/1/2022	3:15:05 PM	11.9211	5.2703	2.4891	14.3892	11.9459	5.2934	2.747	13.0924	25.1	27	21.2
	15	2/1/2022	3:18:46 PM	11.9195	5.271	2.5186	14.2274	11.9495	5.2913	2.6678	13.4641	25.1	27.1	21.2
	16	2/1/2022	3:22:53 PM	14.922	6.6053	2.6294	13.652	14.951	6.6296	2.8248	12.7475	25.1	27.1	21.1
	17	2/1/2022	3:27:06 PM	14.919	6.6043	2.6361	13.6188	14.9504	6.6289	2.818	12.7769	25.1	27.2	21.1
	18	2/1/2022	3:31:09 PM	14.9183	6.6049	2.6516	13.5429	14.9457	6.6267	2.8151	12.7894	25.1	27.2	21.1
	19	2/1/2022	3:35:21 PM	14.924	6.6079	2.6598	13.5026	14.9483	6.6282	2.822	12.7594	25.2	27.2	21.1
	20	2/1/2022	3:39:37 PM	14.9213	6.6047	2.6251	13.6734	14.9462	6.6254	2.79	12.8995	25.2	27.3	21.1

SYSTEM CALCULATED AVERAGES

Average PE-023 Vsh	Average PE-023 Vm	Average PE-024 Vsh	Average PE-024 Vm	Average PE-023 Vpin	Average PE-024 Vpin	Average PE-023 Ppin	Average PE-024 Ppin
59.4622	79.7317	59.7815	79.304	2.3726	2.6408	15.2341	13.6436

Calculated Capsule Volume	2.3726	cc
Calculated Capsule Internal Pressure	15.2341	psia

PE-023 is a 0-15 psia gauge with a +/- 0.05% Full Scale Accuracy

PE-024 is a 0-50 psia guage with a +/- 0.05% Full Scale Accuracy

The results calculated from PE-023 are expected to be more accurate than those from PE-024

The initial capsule fill pressure after welding was 14.955 psia.

The time between charging to 14.955 psia and subsequent drilling and volume analysis was approximately 2 hrs.

HFEF Tracking NO.: 2-5423

Specimen ID: TPRC-04 First Analysis

Specimen Type:	**ATR Salt Radiolysis container**
ID Number:	**TPRC-04**
MTG ID Number:	**TPRC-04**
Diameter:	0.375
Wall Thickness:	0.02
Length:	3.17
DWG Number:	1004226
Estimated Sample Gas Press:	12.2
Aux. Volume:	None
Transducer:	PI-023 (0-15)
Focus Position (Turns):	9.5

Laser Configuration:
Drilling:
Burst 1, .02 inch thick: Pulse Width 750 micro-sec, 1125 mJ, 1500W, 6 pulses.

Welding:
Burst 3, .02 inch thick: Pulse Width 600 micro-sec, 900 mJ, 1500W, 6 pulses.
focus lens at 9.7/.797 inch

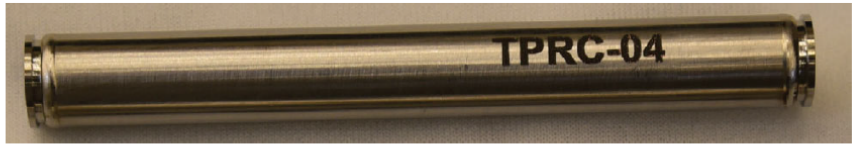

PRE-USE INSPECTIONS

Iteration	Date	Time	Initial PE-023	Final PE-023	Vsh	Vm	Initial PE-024	Final PE-024	Vsh	Vm	TE-044	TE-042	TE-043
1	2/2/2022	7:41:02 AM	4.9229	2.1042	58.9251	80.4556	4.942	2.1228	59.4331	79.7679	23.2	23.9	20.3
2	2/2/2022	7:43:51 AM	6.9227	2.9699	59.3054	79.9397	6.9411	2.9888	59.6928	79.4209	23.3	23.9	20.4
3	2/2/2022	7:47:10 AM	9.9212	4.2686	59.608	79.5339	9.9428	4.2853	59.7901	79.2916	23.3	23.9	20.4
4	2/2/2022	7:50:55 AM	11.933	5.1398	59.7219	79.3822	11.9534	5.159	59.9342	79.1011	23.4	24	20.3
5	2/2/2022	7:55:06 AM	14.9322	6.4369	59.8085	79.2672	14.9568	6.4551	59.9332	79.1023	23.5	24	20.3

POST PUNCTURE AND CAPSULE GAS EXPANSION

Sample	Date	Time	Pex	PE-021	PE-024	PE-026	TE-044	TE-042	TE-043
Puncture	2/2/2022	8:09:10 AM	0.4298	0.4298	---------	---------	23.76	24.14	20.14
Manifold	2/2/2022	8:10:16 AM	---------	0.1598	0.18	-0.1412	23.79	24.2	20.13
Sample Tubing	2/2/2022	8:10:25 AM	---------	0.1605	0.162	-0.1391	23.79	24.21	20.14
Sample Bottle Pressure	2/2/2022	8:10:48 AM	---------	0.1599	0.0446	-0.0791	23.8	24.22	20.14

BACKFILL/EXPANSIONS

Iteration	Date	Time	Initial PE-023	Final PE-023	Vpin PE-023	Ppin PE-023	Initial PE-024	Final PE-024	Vpin PE-024	Ppin PE-024	TE-44	TE-42	TE-43
1	2/2/2022	8:18:36 AM	6.9285	3.0521	2.0872	12.7966	6.9499	3.0713	2.4433	10.994	23.9	24.4	20.2
2	2/2/2022	8:21:30 AM	6.9302	3.0526	2.0781	12.8504	6.9535	3.0694	2.3159	11.5751	24	24.4	20.1
3	2/2/2022	8:24:22 AM	6.9152	3.0455	2.0618	12.949	6.9354	3.0688	2.5866	10.409	24	24.5	20.1
4	2/2/2022	8:26:58 AM	6.9236	3.0498	2.0817	12.8289	6.9438	3.0635	2.2561	11.8706	24.1	24.5	20.1
5	2/2/2022	8:29:51 AM	6.9273	3.0508	2.0588	12.9672	6.9515	3.0708	2.399	11.189	24.1	24.5	20.1
6	2/2/2022	8:33:20 AM	9.9301	4.3843	2.3415	11.4535	9.9504	4.3985	2.4744	10.8614	24.2	24.6	20
7	2/2/2022	8:36:44 AM	9.9278	4.3846	2.3736	11.3042	9.9509	4.4003	2.5154	10.6913	24	24.6	20
8	2/2/2022	8:40:05 AM	9.9284	4.3836	2.3431	11.4457	9.9463	4.4009	2.5811	10.4301	23.6	24.5	20
9	2/2/2022	8:43:21 AM	9.9318	4.3852	2.3463	11.4311	9.9532	4.4021	2.5351	10.6115	23.1	24.4	20
10	2/2/2022	8:46:36 AM	9.9264	4.3824	2.3335	11.4913	9.9469	4.4009	2.5752	10.4529	23	24.3	20
11	2/2/2022	8:50:18 AM	11.9249	5.2689	2.4233	11.0813	11.9468	5.2868	2.5975	10.367	23	24.2	20
12	2/2/2022	8:54:03 AM	11.9301	5.2714	2.4277	11.062	11.9506	5.2886	2.6005	10.3556	23	24.1	20
13	2/2/2022	8:57:47 AM	11.92	5.2668	2.4247	11.0753	11.9453	5.2853	2.5808	10.4311	23.1	24.1	20
14	2/2/2022	9:01:19 AM	11.9183	5.2679	2.4629	10.9098	11.9409	5.2868	2.6535	10.1571	23.2	24.1	19.9
15	2/2/2022	9:05:06 AM	11.9223	5.2705	2.4819	10.8296	11.9439	5.2874	2.638	10.2144	23.3	24.1	19.9
16	2/2/2022	9:09:15 AM	14.9329	6.607	2.5761	10.4493	14.9566	6.6251	2.7064	9.9671	23.4	24.1	19.9
17	2/2/2022	9:13:23 AM	14.9272	6.6054	2.5936	10.3818	14.9464	6.6233	2.7517	9.8099	23.5	24.2	19.9
18	2/2/2022	9:17:33 AM	14.9332	6.6078	2.5874	10.4059	14.9541	6.6247	2.7177	9.9274	23.6	24.2	19.8
19	2/2/2022	9:21:50 AM	14.9261	6.6061	2.6129	10.3083	14.9464	6.625	2.7811	9.7109	23.6	24.2	19.8
20	2/2/2022	9:26:08 AM	14.928	6.6063	2.6013	10.3524	14.9552	6.6217	2.659	10.1369	23.7	24.3	19.8

SYSTEM CALCULATED AVERAGES

Average PE-023 Vsh	Average PE-023 Vm	Average PE-024 Vsh	Average PE-024 Vm	Average PE-023 Vpin	Average PE-024 Vpin	Average PE-023 Ppin	Average PE-024 Ppin
59.4738	79.7157	59.7567	79.3368	2.3649	2.5684	11.4187	10.5081

Calculated Capsule Volume	2.3649
Calculated Capsule Internal Pressure	11.4187

PE-023 is a 0-15 psia gauge with a +/- 0.05% Full Scale Accuracy
PE-024 is a 0-50 psia guage with a +/- 0.05% Full Scale Accuracy
The results calculated from PE-023 are expected to be more accurate than those from PE-024

HFEF Tracking NO.: 2-5423 **Specimen ID: TPRC-04 Second Analysis**

Specimen Type:	**ATR Salt Radiolysis container**
ID Number:	**TPRC-04**
MTG ID Number:	**TPRC-04**
Diameter:	0.375
Wall Thickness:	0.02
Length:	3.17
DWG Number:	1004226
Estimated Sample Gas Press:	14.951
Aux. Volume:	None
Transducer:	PI-023 (0-15)
Focus Position (Turns):	9.5
Laser Configuration:	
Drilling:	
Burst 1, .02 inch thick: Pulse Width 750 micro-sec, 1125 mJ, 1500W, 6 pulses.	
Welding:	
Burst 3, .02 inch thick: Pulse Width 600 micro-sec, 900 mJ, 1500W, 6 pulses.	
focus lens at 9.7/.797 inch	

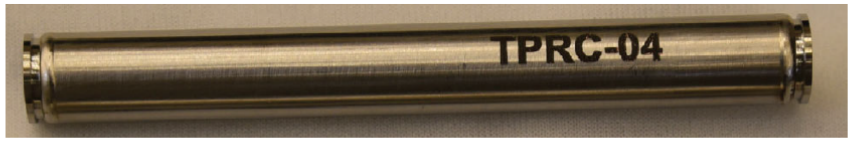

PRE-USE INSPECTIONS

Iteration	Date	Time	Initial PE-023	Final PE-023	Vsh	Vm	Initial PE-024	Final PE-024	Vsh	Vm	TE-044	TE-042	TE-043
1	2/2/2022	1:41:12 PM	4.92	2.1047	59.0087	80.3416	4.9442	2.1231	59.4044	79.8065	23.7	24.1	19.9
2	2/2/2022	1:44:12 PM	6.929	2.9742	59.362	79.8634	6.9507	2.9946	59.7498	79.3451	23.7	24.1	19.9
3	2/2/2022	1:47:43 PM	9.9258	4.2697	59.5859	79.5634	9.9478	4.2876	59.7919	79.2892	23.7	24.1	19.9
4	2/2/2022	1:51:18 PM	11.9215	5.1324	59.673	79.4473	11.9449	5.1543	59.9144	79.1271	23.7	24.1	19.9
5	2/2/2022	1:55:24 PM	14.925	6.4324	59.7863	79.2967	14.9492	6.4548	59.9813	79.0389	23.7	24.1	19.9

POST PUNCTURE AND CAPSULE GAS EXPANSION

Sample	Date	Time	Pex	PE-021	PE-024	PE-026	TE-044	TE-042	TE-043
Puncture	2/2/2022	2:13:15 PM	0.6319	0.6319	---------	---------	23.82	24.16	20.11
Manifold	2/2/2022	2:14:23 PM	---------	0.2519	0.2751	-0.1405	23.82	24.2	20.12
Sample Tubing	2/2/2022	2:14:33 PM	---------	0.2523	0.1224	-0.1265	23.83	24.21	20.12
Sample Bottle Pressure	2/2/2022	2:14:53 PM	---------	0.2529	0.0661	-0.0447	23.83	24.21	20.12

BACKFILL/EXPANSIONS

Iteration	Date	Time	Initial PE-023	Final PE-023	Vpin PE-023	Ppin PE-023	Initial PE-024	Final PE-024	Vpin PE-024	Ppin PE-024	TE-44	TE-42	TE-43
1	2/2/2022	2:20:16 PM	6.9293	3.0519	2.0664	18.998	6.9505	3.0698	2.3793	16.5826	23.9	24.2	20.2
2	2/2/2022	2:23:10 PM	6.919	3.0474	2.0712	18.9556	6.9432	3.0671	2.3982	16.4573	23.9	24.3	20.2
3	2/2/2022	2:26:10 PM	6.9177	3.047	2.0758	18.9151	6.9397	3.0683	2.4973	15.8292	23.9	24.3	20.2
4	2/2/2022	2:29:04 PM	6.9244	3.0488	2.0344	19.2874	6.9478	3.066	2.282	17.2633	23.9	24.3	20.2
5	2/2/2022	2:31:56 PM	6.9171	3.0475	2.1053	18.6593	6.9394	3.0688	2.5201	15.6915	24	24.3	20.2
6	2/2/2022	2:35:26 PM	9.922	4.3804	2.334	16.8927	9.9445	4.4004	2.588	15.2966	24	24.4	20.2
7	2/2/2022	2:38:48 PM	9.9266	4.3828	2.3417	16.8393	9.9508	4.4045	2.6229	15.1015	24	24.4	20.1
8	2/2/2022	2:42:11 PM	9.9228	4.3812	2.3448	16.8179	9.9436	4.4005	2.6028	15.2131	24	24.4	20.1
9	2/2/2022	2:45:33 PM	9.9258	4.3835	2.3682	16.6575	9.9476	4.4027	2.6143	15.1488	24.1	24.5	20.1
10	2/2/2022	2:49:00 PM	9.9152	4.3796	2.3883	16.5229	9.9359	4.3995	2.663	14.8836	24.1	24.5	20.1
11	2/2/2022	2:52:47 PM	11.9228	5.2694	2.454	16.0971	11.9462	5.2911	2.6957	14.7108	24.1	24.5	20
12	2/2/2022	2:56:27 PM	11.9265	5.2715	2.4634	16.0383	11.9488	5.2917	2.6837	14.7736	24.1	24.5	20
13	2/2/2022	3:00:05 PM	11.931	5.2741	2.4767	15.9558	11.9503	5.2943	2.7251	14.5587	24.2	24.6	20
14	2/2/2022	3:03:52 PM	11.9244	5.2714	2.4804	15.933	11.9463	5.2886	2.6419	14.9975	24.2	24.6	20
15	2/2/2022	3:07:41 PM	11.9284	5.2728	2.4736	15.9748	11.95	5.2923	2.6842	14.771	24.2	24.6	20
16	2/2/2022	3:11:58 PM	14.9268	6.6059	2.6046	15.2029	14.9493	6.6238	2.7399	14.4836	24.2	24.6	20
17	2/2/2022	3:16:15 PM	14.9307	6.6088	2.6235	15.0981	14.953	6.6272	2.769	14.3378	24.3	24.7	19.9
18	2/2/2022	3:20:25 PM	14.9313	6.6083	2.6118	15.1631	14.9517	6.6262	2.7617	14.374	24.3	24.7	19.9
19	2/2/2022	3:24:35 PM	14.9314	6.6085	2.6138	15.152	14.9558	6.6258	2.7252	14.5582	24.4	24.8	19.9
20	2/2/2022	3:28:46 PM	14.9221	6.6052	2.6277	15.0752	14.9456	6.6231	2.7557	14.4039	24.4	24.8	19.9

SYSTEM CALCULATED AVERAGES

Average PE-023 Vsh	Average PE-023 Vm	Average PE-024 Vsh	Average PE-024 Vm	Average PE-023 Vpin	Average PE-024 Vpin	Average PE-023 Ppin	Average PE-024 Ppin
59.4832	79.7025	59.7684	79.3214	2.378	2.6175	16.7118	15.1718

Calculated Capsule Volume	2.378
Calculated Capsule Internal Pressure	16.7118

PE-023 is a 0-15 psia gauge with a +/- 0.05% Full Scale Accuracy
PE-024 is a 0-50 psia guage with a +/- 0.05% Full Scale Accuracy
The results calculated from PE-023 are expected to be more accurate than those from PE-024
The initial capsule fill pressure after welding was 14.955 psia.
The time between charging to 14.951 psia and subsequent drilling and volume analysis was approximately 2 hrs.

8. Appendix C: Port City Instruments UV Gas Spectrometer User Guide

INL Chlorine Gas Monitor (2021)

User Guide

Rev. A, September, 2021

Port City Instruments, LLC
8110 S Houghton Rd, Ste 158-180
Tucson, AZ 85747 USA
Tel: +1 520-262-9414

Table of Contents

1) Introduction

This document describes operational procedures for a UV LED based chlorine gas monitor built for Idaho National Laboratory. It directs a 325 nm LED through a multipass White cell (5m optical path) and to a 5 mm diameter silicon detector mounted to the exit port of the White cell. The White cell was provided by PIKE Technologies and was ordered directly from them by INL. Port City Instruments incorporated this White cell into an assembly with the LED and detector, and provided the control electronics and an example control program with GUI (source code provided to INL).

2) Initial Set Up

The system consists of two separate modules. One is the main control electronics box with internal power supply and a data acquisition module. This box has a power entry module on the rear panel for standard 120 VAC, 60Hz wall power, and a rear panel fan which as been disconnected (it is not needed). The front panel has a standard USB port for connection of the data acquisition module to a PC, and a 9-pin Dsub connector (pinout in Appendix A) for the main cable between the control electronics box and a much smaller (red) electronics box mounted on the second module. A standard "modem" cable (pins wired straight through, ie. 1-1, 2-2, etc.) is included, as well as a 120 VAC power cable and a USB cable.

The second module is a 6 x 12" Al base plate with the PIKE White cell mounted in the center. A

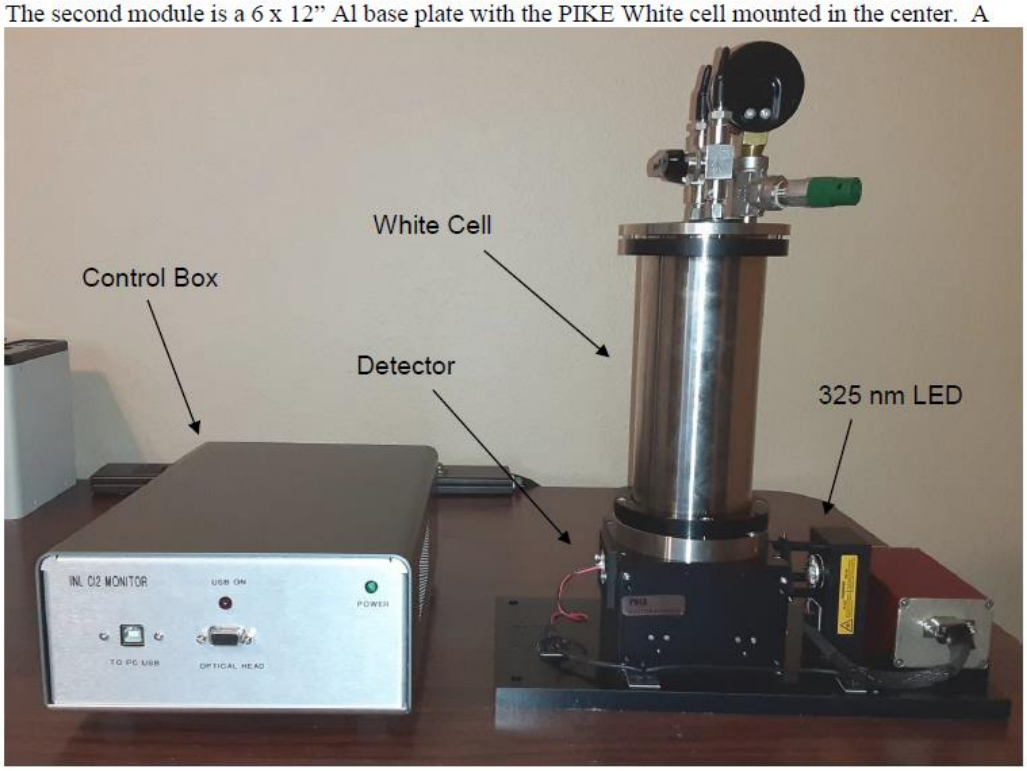

small, red electronics box is mounted on this base plate next to the LED mount and heat sink. This box mates to the main control box via a 9-pin D cable (wired straight through, no crossovers). It also has a second 9-pin D connector which mates to the LED and detector. The red box contains circuitry to drive the LED (square wave chop at ~1450 Hz) and the preamp.

To set the system up, do the following steps in the order shown:

1) Install the Dataq software (.exe file in the root directory of the USB stick). This has the necessary drivers and DLLs for the 16-bit I/O module (Dataq model DI-2108-P) inside the main control box, which also contains at triple output power supply (+5V, ±12V).

2) Copy the VB_GUI directory on the USB stick to any directory on the PC hard disk. This has the VB.Net project file (the .sln solution file) that can be opened in Visual Studio 2017 or later. There is also a "publish" directory which contains the installer files created from within Visual Studio (see the supplied videos on the GUI).

3) Create a director on the PC hard disk called C:\Temp. Or, open the .sln project file in Visual Studio and change this directory name in the source code if you want another name. It is used to write some diagnostic files (which can be disable once things are working OK).

4) Mount the White cell base in its target location and connect the flow ports. PIKE supplied some blue tubing, but I'd guess you want SS or monel or something more sturdy.

5) Position the main control box as close as possible to the White cell and connect the power cable to a standard 120VAC outlet, and connect the supplied 9-pin D cable between the main control box and the small red box on the White cell base (which contains the LED driver, and the preamp). Connect the supplied USB cable between the main control box and a PC (or connect this when you are ready to start up and run tests).

6) Ground the White cell body or the lower attachment screws to the GND hex standoff on the small, red box. This grounding point is a little too close to the 9-pin D cable's strain relief on the red box, but the cable will fit with a little effort. I simply ran a clip lead from one of the 4 lower attachment screws on the White cell to this hex standoff, but a more permanent approach may work better. It is necessary to ground the White cell body to the red box ground standoff to minimize 60 Hz pickup and overshoot/undershoot of the signals from the high-gain preamp.

7) Turn the LED on using the ON/OFF switch on the rear panel of the main control box. The Dataq I/O module is powered from the USB port, while the LED driver and preamp are powered from the internal power supply in the main control box. So this rear panel switch basically just turns the LED on and off. Always keep this off when not making measurements to maximize the life of the LED. These are spec'd at about a 5000 hour nominal lifetime.

8) See the provided two videos (screen recordings) for details on the GUI operation.

The Dataq module has 8 analog input channels and 8 digital I/O channels. At present, only a single

analog input channel (channel 1) is connected to the preamp output, but an additional 7 analog input channels are available for expansion. There are also 8 digital I/O lines currently unused that can be allocated to various functions if desired. These extra analog and digital inputs are supported by the example test program as far as their definitions, so can be implemented with minor code changes. For example, they could be used to trigger acquisition, synch with mass flow controllers, etc.

3) Making Measurements

Gas phase Cl_2 has an absorption band near 325 nm in the UV (see cross section plot next page, (from D. Maric, J.P. Burrows, R. Meller, G.K. Moortgat, *J. Photochemistry and Photobiology A: Chemistry*, Vol 70, Issue 3, 1 March 1993, Pages 205-214).) which can be used to monitor concentrations of Cl_2 using the measured absorption at 325 nm via the Beer-Lambert law:

$$T = \exp(-k(\nu)*\rho*L) \quad (1)$$

where T (transmission) is equal to I/Io which is the ratio of transmission through the White cell with no Cl_2 present (Io) and with Cl_2 present (I), $k(\nu)$ is the absorption cross section in cm^2/molecule and is a function of wavenumber (ν) as well as pressure and temperature, ρ is the number density of Cl_2 in molecules/cm^3, and L is the optical path length in cm. Absorption (A) = 1 - T. For small levels of absorption (below 10%) , $A \sim k(\nu)*\rho*L$ (because when x is small, $\exp(-x) \sim 1-x$), or $\rho \sim A / (k(\nu)*L)$. This approximation introduces less than a 1% error in the derived gas number density at A = 10%, and negligible error below A=2%. Once ρ is known, it can be converted to other units such as parts per million by volume (ppmv) by dividing by the total number density for the measurement conditions. Total number density, N, can be gotten from Loschmidts number with adjustments for pressure and temperature (N is in molecules/cm^3):

$$N = 2.6868e19 * (P/1013.2) * (273.15/T) \quad (2)$$

where P is the measurement pressure in mbar and T is the measurement temperature in Kelvin. So to convert a measurement of molecules/cm^3 to ppmv, simply evaluate Eqn. 2 for the measurement conditions (P and T), and evaluate:

$$ppmv = (\rho / N) * 1e6 \quad (3)$$

A sample PC program with GUI is provided for initial use, along with the source code written in VB.Net using Visual Studio 2017. It can be modified as needed by INL. Two short videos are provided to illustrate the GUI operation, which is set up for manual recording of background and measurement signals in sequence. These can be recorded in either order, with multiple recordings of each independently as illustrated in the videos.

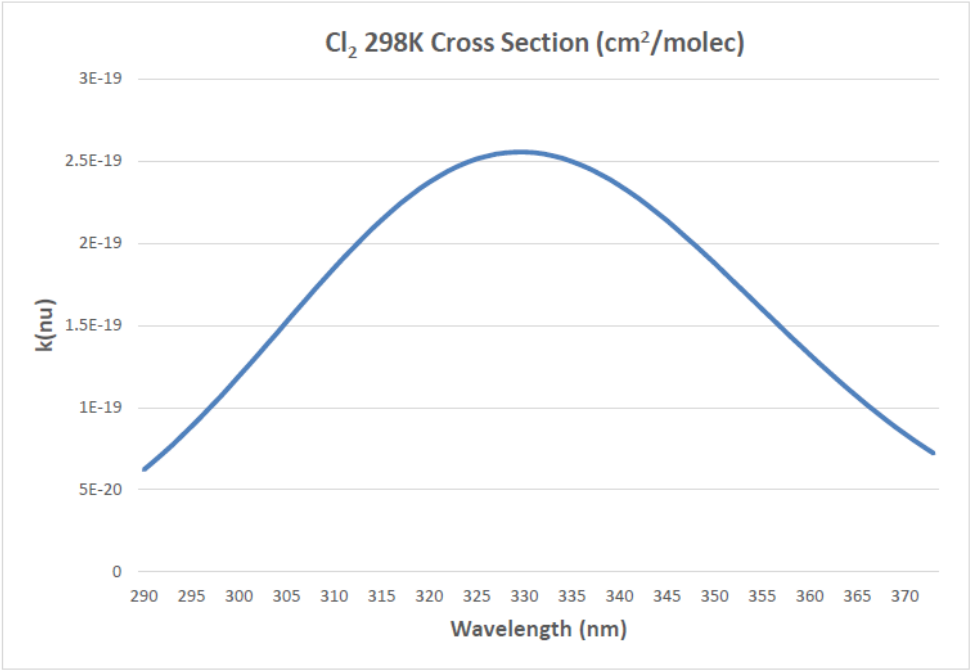

4) Software Operation

The source code for the example program is a VB.Net program modified from a demo program that Dataq provide with their I/O modules. Its operation is described in two .MP4 video files so won't be described in detail here apart from a few comments.

Since the measurements are described as being done manually (background gas with no Cl_2, then a measurement scan with Cl_2), a "latch" scheme has been implemented. Either a background or a measurement acquisition can be done at any time. There are two "Select" option buttons in the center section of the GUI (again, see the videos provided). These select either Measurement or Background for the next acquisition. Once the desired measurement is selected, click the START button between the two Select options.

When this is done, the START button will change to LATCH and the Datag I/O module is read for 2s. Progress is shown in the rightmost text window on the GUI, and when completed a message appears "OK to latch" at the bottom of this text window (wait for that to happen). At this point the LATCH button is clicked which processes the square wave signal from the preamp (the LED is square wave chopped at ~1450 Hz) and fills in the numbers for that side of the GUI. Repeat for the other measurement (Background or Measurement) and when both are recorded the Cl_2 number

density should have a valid value. The CLEAR button zeros all the numbers and a new measurement can be taken. It doesn't matter which order the Measurement and Background are taken, or how often they are initiated in a row. The software just uses the most recent values in the text boxes for the calculation, and these raw data test boxes are updated at each new START/LATCH cycle.

The source code can be edited to configure this as needed at INL. This program was meant only as a template with the core functions needed to acquire the data and calculate the Cl_2 number density. File writing and many other functions can be added, pressure and temperature sensors, triggers, etc. using the extra analog and digital channels available on the Dataq module.

5) Calibration

This software is currently set up with a simple Beer's law calculation of the Cl_2 number density, and uses the maximum cross section at 325 nm. The LED may not be centered exactly at 325 nm, and it is not a narrow linewidth laser so the integrated cross section will most likely be different that the default value used in the software. This can be measured directly via a known amount of Cl_2 by simply scaling the reported Cl_2 number density with the known value. For example, If 100 ppmv Cl_2 were added to the cell at 500 mbar total pressure and 296K the number density of Cl_2 would be (from Eqn. 2):

$$N(Cl_2) = 2.6868e19 * (500/1013.2) * (273.15/296.0) * 100e\text{-}6 = 1.22e15/cm^3$$

If the GUI were to read 1.55e15 (a factor of 1.27 too high) with the cross section set to 2.48e-19, then the adjusted cross section would be:

$$k(\nu) \text{ calibrated} = 2.48e\text{-}19 * (1.55e15 / 1.22e15) = 3.15e19 \text{ cm}^2/\text{molecule} \qquad (4)$$

as the cross section appears in the denominator of the equation for number density ρ:

$$\rho \sim A / (k(\nu)*L) \qquad (5)$$

and increasing $k(\nu)$ would decrease the reported number density in proportion. There are also slope and intercept values on the GUI for a linear zero/span type of calibration. This is currently implented in the code as:

$$Cl_2(\text{new}) = \text{intercept} + \text{slope} * Cl_2(\text{old})$$

6) Contact information

If there are any problems with the spectrometer contact Randy May at Port City Instruments, LLC between 8:00 am and 6:00 pm Pacific Time, any day of the week:

Email:	randy@portcityinstruments.com
Telephone:	+1 520-262-9414 (Cell)
Shipping Address:	8110 S Houghton Rd. Ste 158-180 Tucson, AZ 85747 USA

Appendix A – Connector Pin outs

NOTE: The 9-pin D (both sides) cable between the main control box and the small, red box on the White cell base is a "modem" cable with the pins wired 1-1, 2-2, 3-3, etc. (ie. straight through with no crossovers)! So-called "null modem" cables have certain lines crossed internal to the cables so be sure **NOT** to use that type of cable if a different length is needed than the one provided. If INL make a new cable for this, just wire pin 1 on one side to pin 1 on the other side, and the same for all other pins. The cable has a female on one side and a male on the other, so it can be connected only one way between the two boxes. The other 9-pin D cable on the small, red box mates to the LED and this cable was intentionally made too short to reach the opposite side of the red box.

The connector pinouts are given below:

Main Control Box (9-pin Dsub female, and Red Box 9-pin Dsub male)

(*Note: Cable from main control box to red driver box is wired straight through*)

Pin	Signal
1	+12V
2	-12V
3	Preamp Output
4	N/C (no connection)
5	N/C (no connection)
6	Ground
7	Ground
8	+5V
9	+5V

Red Box to LED and Detector (9-pin Dsub female)

Pin	Signal
1	LED + (anode)
2	LED - (cathode)
3	N/C (no connection)
4	TEC+ (not installed for INL)
5	TEC- (not installled for INL)
6	Thermistor 1
7	Thermistor 2
8	Det - (cathode)
9	Det + (anode)